ELSEVIER

Polymer 40 (1999) 1279–1297

polymer

Poly(amidoamine) hyperbranched systems: synthesis, structure and characterization

Lois J. Hobson, W. James Feast*

Interdisciplinary Research Centre in Polymer Science and Technology, University of Durham, Durham DH1 3LE, UK

Received 16 February 1998; accepted 26 March 1998

Abstract

Hyperbranched analogues of the Tomalia PAMAM dendrimer system have been prepared from a series of AB_2 aminoacrylate hydrochloride monomers using Michael addition chemistry, where A represents a Michael acceptor and B_2 a primary aliphatic amine. This step-growth polymerization process has led to the synthesis of poly(amidoamine) hyperbranched materials, examples of which exhibit a branching factor close to one. This degree of branching, calculated from quantitative ^{15}N NMR spectroscopy data, is consistent with other spectroscopic characterization undertaken and the assignment of the ^{15}N NMR shifts observed correlates well with the available literature data. The use of MALDI-TOF mass spectrometry as a tool to evaluate the possibility of intramolecular cyclization reactions between the focus and terminal groups is discussed along with the determination of molecular weights and molecular weight distributions for these amidoamine hyperbranched polymers. The synthesis of pseudo-dendrimers through 'one-pot' AB_2/B_n copolymerizations, where control over both molecular weight and extent of branching through the B_n unit is illustrated. A poly(amidoamine) hyperbranched AB_2/B_6 copolymer is shown to display a viscosity/molecular weight profile similar to that exhibited by dendrimers. The effect of varying the internal spacer unit length between the branch points A and B is discussed, with reference to both the standard AB_2 polymerizations and the core terminated AB_2/B_n copolymerizations. Preliminary physical characterisation (T_g, DSC and solution viscosity) of these novel materials is reported.

Keywords: Hyperbranched; Poly(amidoamine); MALDI-TOF

1. Introduction

Synthetic organic polymers, although of enormous importance in many technologies, are relatively young materials. Many applications have been developed in an empirical manner and, in view of the complexity possible, it is not surprising that the detailed correlation of properties with structure is inadequately understood for many polymeric materials. Structure in this context is, of course, a portmanteau word including everything from atomic connectivity through to the relative dispositions and interactions of various domains in the supramolecular organisation of the material. For most of the last fifty years scientists concerned with the synthesis and use of organic polymers have concentrated their efforts at the two extremes of the spectrum of possible polymeric materials; namely, essentially linear structures and cross-linked networks. More recently considerable interest has developed in unusual polymer topologies, including rods [1], ribbons [2], rotaxanes [3], dendrimers [4–6] and other branched structures [7–9]. In this new departure for polymer science, work has been focused on making and studying well-defined materials. This, in its turn, generated the requirement for organic syntheses of a complexity and sophistication not normally associated with polymer synthesis. One consequence of this is that many of these newer materials are likely to be costly and their applications limited to the kinds of technologies usually associated with medicine or specialized electronics where such high costs might be tolerated. This is unfortunate because some of these newer materials display properties which may have implications for processing or bulk applications. Consider, as an example, the relationship between molecular weight and viscosity shown schematically in Fig. 1.

For conventional linear polymers (Fig. 1a) the behaviour is accounted for by the Mark–Houwink relationship [10] whereas well-defined monodisperse dendrimers show a viscosity/molecular weight relationship which passes through a peak in viscosity with increasing molecular weight [11]. This behaviour has been said to be a

* Corresponding author.

0032-3861/98/$ - see front matter
PII S0032-3861(98)00268-7

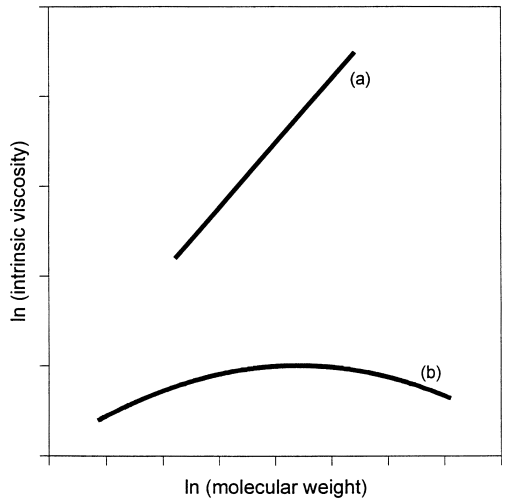

Fig. 1. Schematic representation of solution viscosity/molecular weight relationships for (a) linear and (b) dendritic polymers.

characteristic signature of dendrimers [12] and is potentially attractive from a polymer processing point of view. Thus, all other things being equal, it would be convenient to be able to control the viscosity/molecular weight relationship for a material between the boundaries set by these two lines through regulation of the molecular structure. In this paper we report the use of a relatively simple synthesis to produce materials which to some extent mimic the properties of dendrimers.

Hyperbranched polymers, derived from AB_x units where $x > 1$, can be prepared in a 'one-pot' reaction from appropriately functionalized monomers. This single step approach is in direct contrast to the iterative sequence of reaction and purification steps involved in the synthesis of perfect dendrimers. To generate an AB_2 hyperbranched structure the monomer contains one A and two B groups which under the polymerization conditions react together to produce a highly branched polymeric wedge, Fig. 2. In the ideal case considered by Flory [13], the only **A** group remaining is held at the focus, while the wedge is made up of a number of differently linked **B** groups, including linear, terminal and branched units, see Fig. 2. The relative

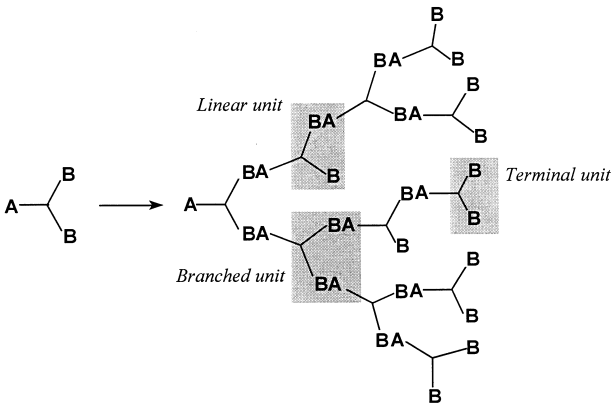

Fig. 2. Schematic representation of an AB_2 polymer.

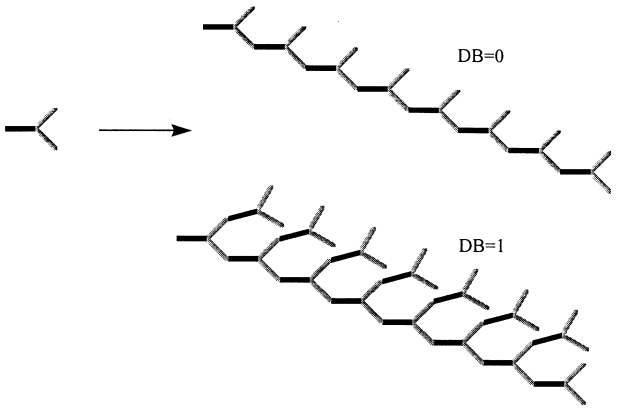

Fig. 3. Possible AB_2 structures.

abundance of linear, terminal and branched units within a polymer is characterized by the degree of branching (DB); zero for linear polymers and one for perfectly branched structures. Since Fréchet's initial definition of DB as the ratio of the sum of branched and terminal repeat units to the total number of repeat units [14], the term has been reconsidered by Frey and coworkers [15] whose calculations take into consideration the fact that a monomer unit has terminal groups and hence under Fréchet's definition contributed towards the number of fully branched species. Their new definition defines DB as the ratio of twice the number of branched units to the sum of twice the number of branched units and the number of linear units. Statistically ideal AB_2 hyperbranched systems are predicted to have a DB of 0.50, under standard one-pot reaction conditions, assuming the B groups are of equal reactivity independent of structure and location [16].

Although control over DB is attractive, this term does not provide useful information about the overall topology of hyperbranched polymers; thus, a DB of 1.0 does not necessarily imply perfect dendritic architecture, merely the absence of linear sections within the structure. For example, it is theoretically possible to construct an essentially linear polymer with DB = 0 or DB = 1, Fig. 3. While at the other extreme, DB = 1 can also be associated with either perfect

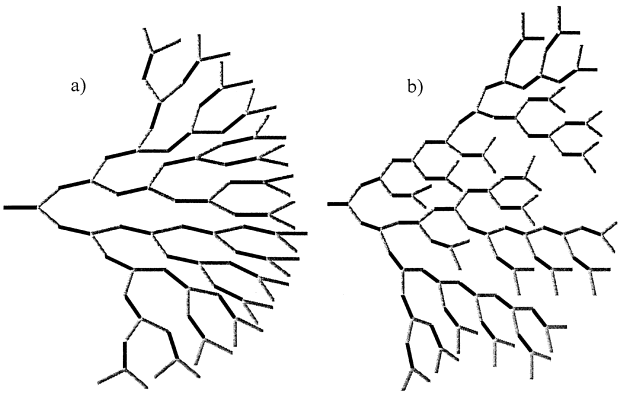

Fig. 4. (a) Perfect branching, regular growth pattern; (b) perfect branching, irregular growth pattern.

dendritic architecture, i.e. perfect branching and perfect growth (Fig. 4a), or a perfectly branched structure with irregular growth (Fig. 4b). Clearly in the range $0 < DB < 1$ there will be an enormous variety of possible topologies. Statistical AB_2 systems were the subject of detailed theoretical analysis by Flory in the 1950s [13], but the experimental exploration of their physical properties and their industrial exploitation are relatively undeveloped.

2. Results and discussion

2.1. Synthesis of monomers and preliminary polymerization studies

Amidoamine hyperbranched polymers have been prepared by addition polymerization in the melt from a series of AB_2 monomers (Fig. 5). The monomer is an ammonium salt but we believe, see below, that the addition step occurs through the free base and that the acrylamide **A** group acts as a Michael acceptor and the **B** group is an N–H bond [17,18]. In the case where $n = 2$ this system represents the hyperbranched analogue of Tomalia's poly(amidoamine) dendrimer system [19].

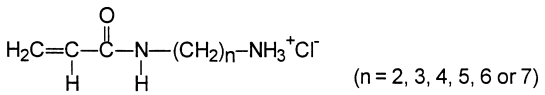

Fig. 5. Monomer structure.

The selective monoacylation of diaminoalkanes has been shown to be unfavourable [20]; consequently the synthesis of these monomers involves classical protection/deprotection chemistry, using the *t*-butoxycarbonyl (*t*-BOC) protecting group [21], as shown in Fig. 6 (see experimental section for details). From the corresponding α,ω-diaminoalkanes the mono-protected intermediates (*N*-*t*-butoxycarbonyl-α,ω-diaminoalkanes) were prepared prior to the introduction of the acrylate functionality at the site of the free amine, by reaction with acryloyl chloride in the presence of triethylamine, followed by deprotection [22] and isolation as the hydrochloride salt. This general method allowed the synthesis of a series of AB_2 aminoacrylate monomers with increasing internal CH_2 spacer length. Melt polymerization occurs via addition of the amine group across the double bond of the acrylate functionality. A 1:1 addition gives a linear unit while 2:1 addition gives the branched structure, Fig. 7.

Trial polymerizations were carried out using the potential monomers derived from 1,6-diaminohexane. Our first approach was to generate the free base, *N*-acryloyl-1,6-diaminohexane, this oil polymerizes on heating under nitrogen to give an insoluble product which we could not characterize adequately. A solution of the free base in D_2O also polymerizes slowly on standing as revealed by ^1H NMR spectroscopic analysis. In our second attempt we used the fact that the *t*-BOC protecting group is reported to be cleaved thermally at temperatures above 185°C [23] and investigated the possibility that this would be a convenient way of generating pure monomer in situ. However, this procedure also gave an insoluble product and elemental analysis showed that the *t*-BOC protecting group was not totally eliminated even after heating at 210°C for 6 h. By contrast heating the pure hydrochloride salt, *N*-acryloyl-1,6-diaminohexane hydrochloride, which melts at 165°C [22], between 190 and 230°C resulted in consumption of the acryloyl group and formation of new methylene units as revealed by FTIR, ^1H and ^{13}C NMR spectroscopies. The product was soluble in water and methanol and characterizable. Below the melting point there was no evidence of polymerization, for example the salt can be recovered unchanged after boiling in aqueous solution. The polymer product has the same elemental composition as the monomer thus no hydrogen chloride is lost during polymerization; however, the alkyl ammonium ions are insufficiently nucleophilic to participate in Michael addition and we presume that the growth process involves addition of the free amine to the acryloyl unit, see below. As a result of these preliminary experiments we adopted standard conditions for the polymerization; namely, heating the hydrochloride salts under an atmosphere of nitrogen at a rate of 10°C min^{-1} to

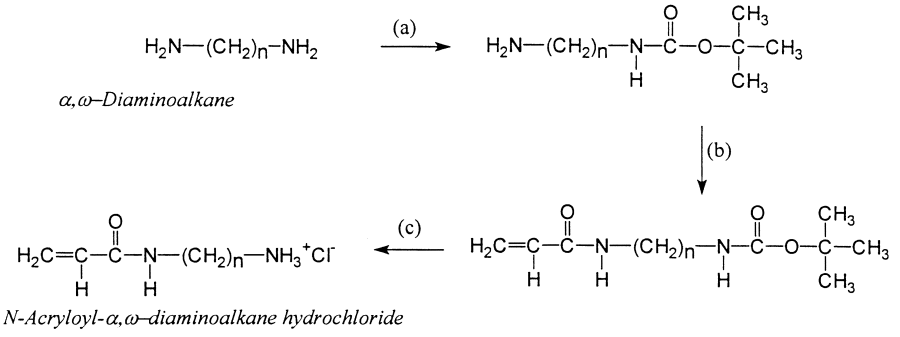

Fig. 6. Synthesis of aminoacrylate monomers. (a) S-*tert*-butoxycarbonyl-2-mercapto-4,6-dimethyl pyrimidine/dioxan [22] or *tert*-butyl dicarbonate/dichloromethane. (b) Acryloyl chloride/triethylamine/chloroform (0 to −10°C). (c) Hydrochloric acid/ethyl acetate.

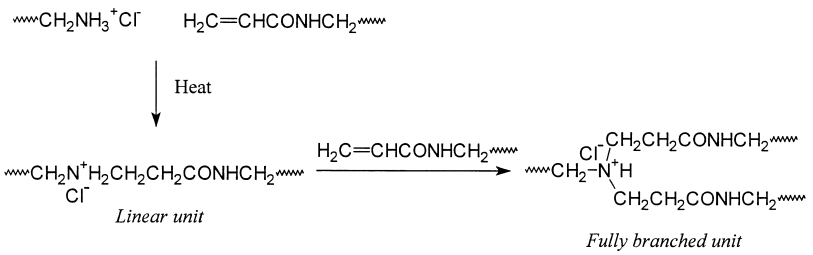

Fig. 7. Polymerization process.

210°C in an apparatus designed to ensure efficient mixing. The duration of reaction was varied between 30 min and 24 h. This protocol allowed the preparation of a series of oligomers and polymers in which the extent of reaction was varied and which gave an opportunity to study reactivity as a function of monomer structure. The mass recovery from the polymerization vessel was essentially 100% in all cases.

2.2. Polymer characterization

The AB_2 poly(amidoamine) hyperbranched wedges are isolated directly from the melt as their amine hydrochloride salts, elemental analysis indicating an approximate composition of one HCl group for every polymer repeat unit. The products are water soluble polyelectrolytes and have been characterised by ^1H, ^{13}C and ^{15}N NMR; IR; elemental analysis, MALDI-TOF and electrospray mass spectrometry, GPC, DSC, TGA, and dilute solution viscometry in order to establish their structures and gain insights into structure/property correlations.

The fact that polymerization occurs by addition of an NH bond across the acrylate double bond is clearly established by IR, ^1H and ^{13}C NMR spectroscopies. The nature of the information available from ^{13}C NMR spectroscopy is illustrated in Fig. 8 where the spectrum of the monomer, *N*-acryloyl-1,6-diaminohexane hydrochloride, is compared with that of the derived polymer. The assignment of the monomer spectrum, Fig. 8a, is straightforward with six methylene, two vinyl and one carbonyl signals. In the polymer spectrum, Fig. 8b, the vinyl signal intensity has dramatically decreased and new methylene carbon signals, confirmed by DEPT [24], consistent with the proposed polymerization pathway, are seen.

Similarly comparison of the IR spectra of this pair of materials shows that the out-of-plane bending modes at 995–985 and 940–900 cm^{-1} in the monomer vinyl unit disappear in the spectrum of the polymer. Consistent with the proposed process, the polymer spectrum shows broader bands than the monomer spectrum and in the 1500–1700 cm^{-1} region three relatively sharp bands in the monomer spectrum at 1528, 1620 and 1662 cm^{-1} are replaced by two broad bands at 1556 and 1651 cm^{-1}.

Examination of the ^1H NMR spectra of the same monomer/polymer pair, Fig. 9, allows confirmation and quantification of the conclusions drawn from the ^{13}C NMR and IR spectra. The assignment of the monomer spectrum, Fig. 9a, is straightforward and it is clear that in the polymer, Fig. 9b,

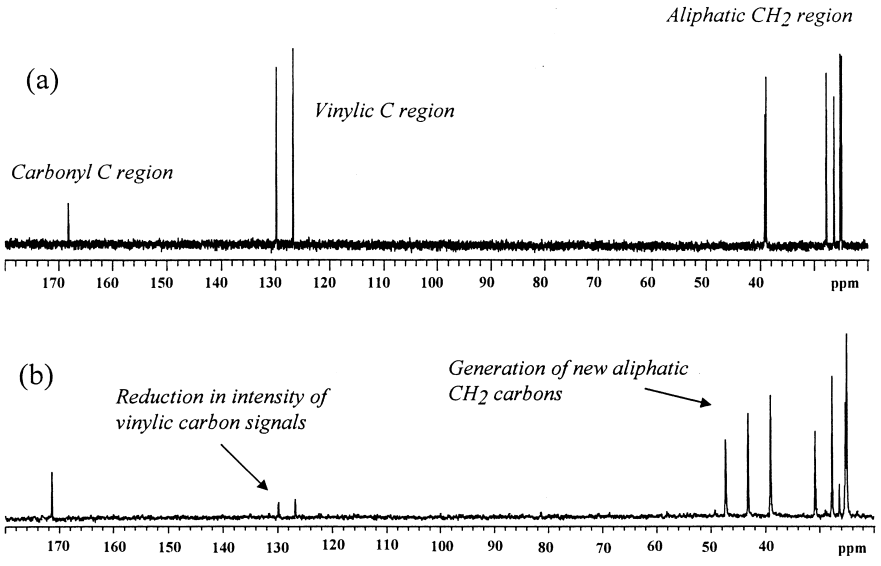

Fig. 8. ^{13}C NMR spectra (D_2O): (a) *N*-acryloyl-1,6-diaminohexane hydrochloride, $n = 6$ (monomer); (b) polymer prepared from *N*-acryloyl-1,6-diaminohexane hydrochloride, by reaction at 230°C for 4 h.

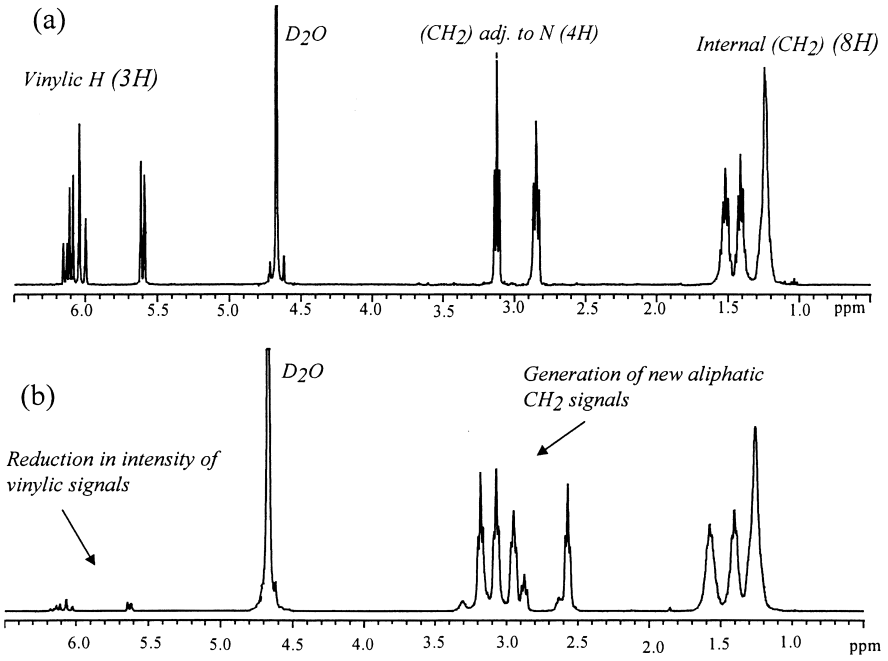

Fig. 9. ^{1}H NMR spectra (D_2O): (a) *N*-acryloyl-1,6-diaminohexane hydrochloride, $n = 6$ (monomer); (b) polymer prepared from *N*-acryloyl-1,6-diaminohexane hydrochloride, by reaction at 230°C for 4 h.

the vinylic signal intensity has decreased and new methylene signals have appeared which confirm the structural deductions discussed above. Comparison of the integrated intensity of the vinylic hydrogens at the focus of the wedge (5.50–6.30 ppm) with that of the methylene hydrogens detected between 1.00 and 2.00 ppm allows the calculation of the extent of consumption of vinyl units and, assuming no ring formation, the degree of polymerization and number average molecular weight. We have used this chain end counting approach to measure M_n for a series of polymers prepared from the six monomers described earlier and have obtained values for M_n in the range 1500–21 000 depending on monomer structure and duration of reaction. Clearly, the higher the M_n value the less reliable the analysis; in our hands the highest M_n which could be determined was 21 000. If termination of polymer growth occurs through cyclization, a recognized phenomena in AB_2 polymerizations [25–27], this analysis would give an optimistically high value of M_n. However, cyclization for these AB_2 systems is ruled out by MALDI-TOF MS anaylsis (see below).

By varying the period of reaction we can establish a relationship between time and extent of reaction, the same data can be presented in terms of degree of polymerization and/or number average molecular weight; Fig. 10 illustrates the data obtained. Thus, in Fig. 10a we see that the extent of reaction, under the same conditions, is a sensitive function of monomer structure. Clearly the monomer derived from ethylenediamine ($n = 2$) reacts faster than that derived from 1,4-diaminobutane ($n = 4$) which in turn reacts significantly faster than that derived from 1,6-diaminohexane ($n = 6$). Fig. 10b illustrates the growth of molecular weight under these conditions for the 1,4-diaminobutane derived monomer. The monomers with odd methylene spacer chains were only studied in a few experiments, because the diamine starting materials are expensive, but the limited data obtained fits the general trends shown in Fig. 10a.

The data presented above show that reactivity in this polyaddition is a function of monomer structure and that the longer the methylene spacer unit sequence the less reactive the monomer. The other interesting feature of the reaction is the complete retention of hydrogen chloride during reaction of a quaternary ammonium chloride in the melt under a stream of nitrogen or under vacuum (10 mmHg). We assume, because it is inherently unlikely that the ammonium ion can act as a nucleophile, that there must be a low concentration of free amine groups instantaneously present during the attack of nitrogen at the vinylic methylene. We postulate that the conformation of the monomer allows the positive nitrogen ($-CH_2NH_3^+Cl^-$) to interact with the amide oxygen as shown schematically in Fig. 11 [28]. When the proton is nearer the carbonyl oxygen the amine is a powerful nucleophile and can participate in Michael addition with an acryloyl unit activated by the same conformational association of ammonium ion and acryloyl carbonyl.

This hypothesis allows us to account for the complete retention of hydrogen chloride during reaction. Ab initio molecular orbital calculations at the RHF321G level were carried out in an attempt to provide support for this hypothesis [29]. The calculations showed that the minimum energy conformation was the cyclic one in which the ammonium ion approached the carbonyl of the acryloyl unit and the maximum energy conformation was that of a fully extended chain. The same conclusions resulted from calculations based on the monomers with 2, 4 and 6 methylenes in the

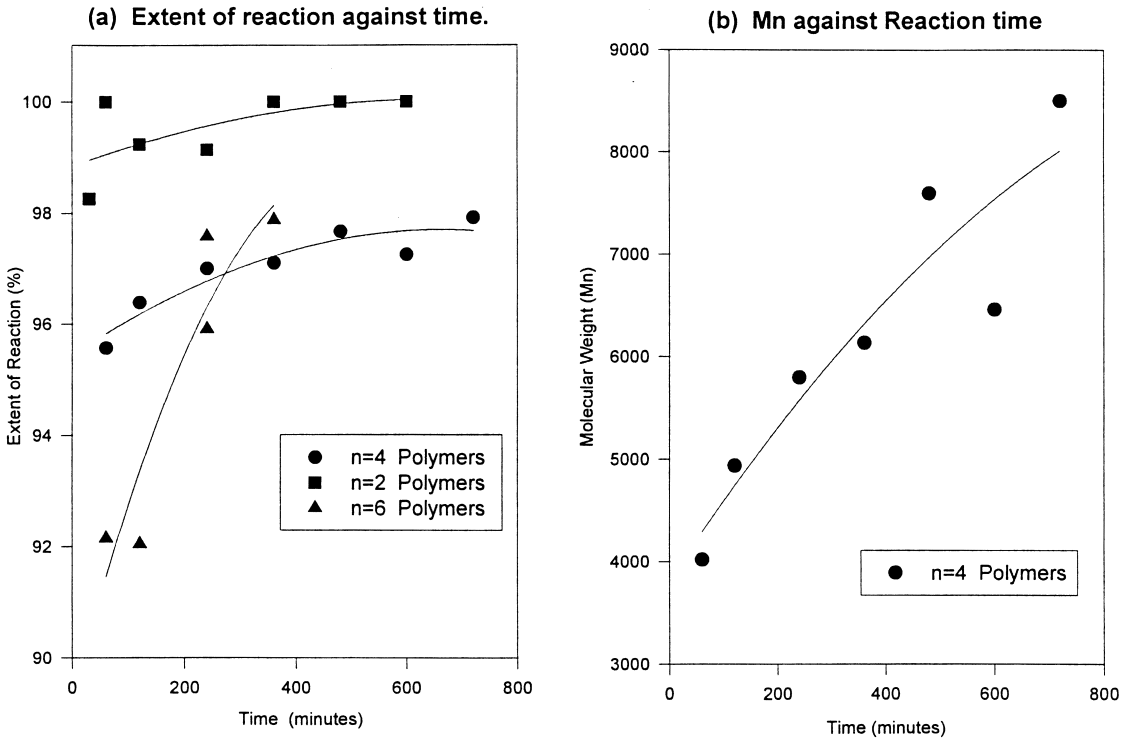

Fig. 10. Graphs to illustrate variation of extent of reaction and molecular weight (calculated from ^{1}H NMR data) as a function of reaction time for reactions conducted on a 4 g scale in the melt at 210°C under nitrogen with efficient stirring.

spacer unit. The energies, energy barriers and charge distributions were similar for all monomers investigated and so if there is any rationalization of the differences in the rate of reaction of the different monomers to be made on the basis of this hypothesis it has to reside in entropic rather than enthalpic or charge distribution effects. This analysis is, of course, consistent with the observation that the monomer with of the shortest methylene chain reacts fastest.

2.3. Cyclization and degree of branching

Analysis of the ^{13}C NMR, ^{1}H NMR and IR spectra establishes that these products arise by addition across the acryloyl double bond, this could result in essentially linear polymers, hyperbranched polymers with varying degrees of branching and/or cyclized versions of these two. It also establishes the relative reactivity of the monomers. In this section we show that analysis of MALDI-TOF mass spectra and ^{15}N NMR spectra allow us to rule out cyclization as a significant reaction pathway and to establish that the degree of branching, like the reactivity, is a sensitive function of monomer structure.

Soft ionisation mass spectroscopy techniques have made a valuable contribution to investigations of polymers [30,31]. We have examined both electrospray and MALDI-TOF techniques and although electrospray allowed us to identify sequences of masses from monomer to simple addition products with DP up to 25, the signal to noise ratio we obtained was poor and the spectra showed significant fragmentation. MALDI-TOF data were clearer and more readily interpreted in detail. Spectra were generated using the Kratos Kompact MALDI IV instrument, operated in linear detection mode to generate positive ion spectra, this instrument has a non-variable accelerating voltage of 18 kV. Generally samples were analysed as their hydrochloride salts (2 mg ml^{-1}, water), using 2,5-dihydroxybenzoic acid (10 mg ml^{-1} [40:60] water/acetonitrile) as the matrix but detected as adducts of the corresponding free bases.

Use of MALDI-TOF mass spectrometry to evaluate the possibility of intramolecular cyclization reactions between the focus and terminal groups has previously been described for hyperbranched polyesters [27,32]. For this particular system, analysis is more complex as no condensate molecule is eliminated upon polymerization via Michael addition chemistry and therefore cyclic oligomers and polymers do not give rise to an independent series of ions. Series of spectra were recorded for the AB_2 polymer systems derived from the set of monomers (n = 2–7). A typical example of a spectrum, recorded for a polymer derived from *N*-acryloyl-1,6-diaminohexane hydrochloride (n = 6), is shown in Fig. 12. There are clearly two series of peaks of

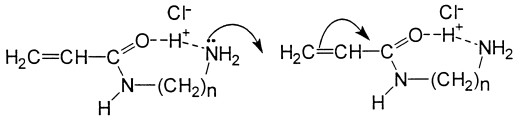

Fig. 11. Proposed mechanism for polymerization.

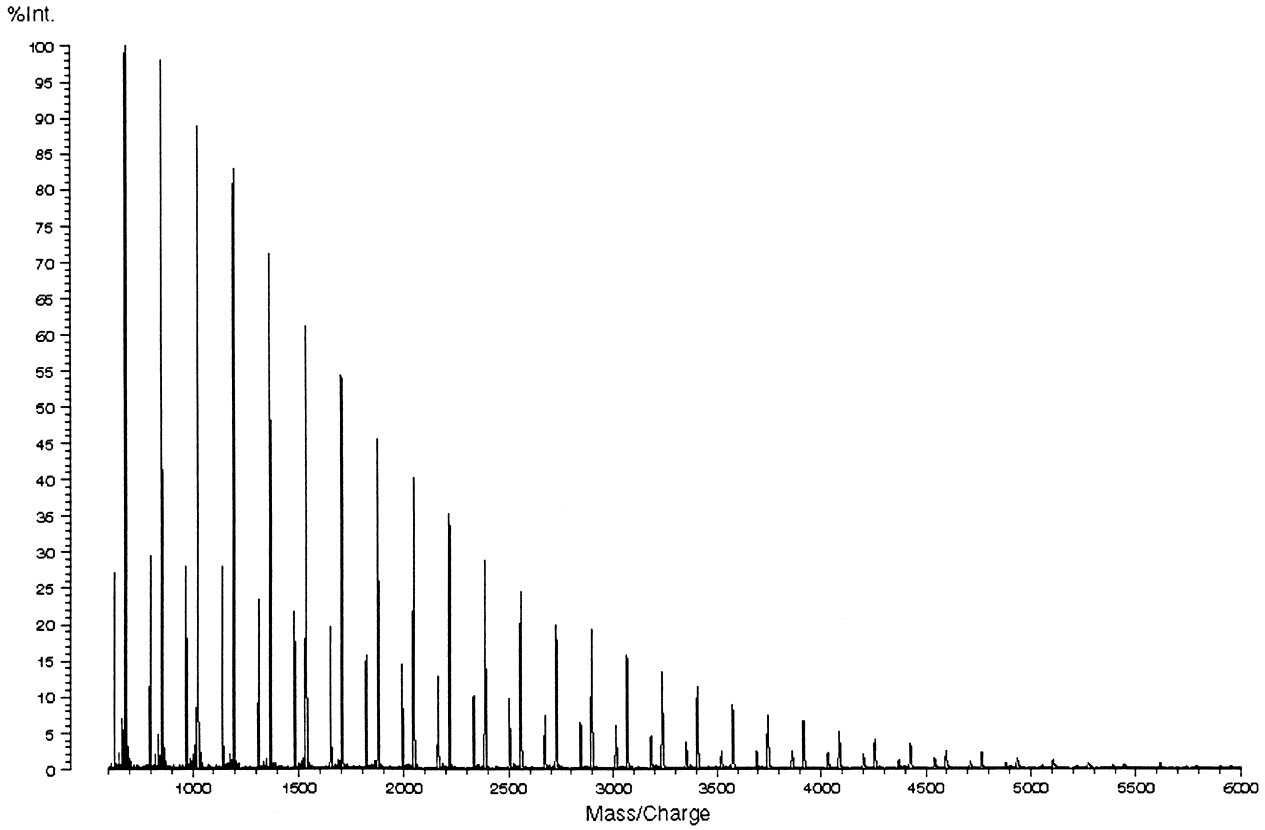

Fig. 12. MALDI-TOF mass spectrum of the polymer prepared from *N*-acryloyl-1,6-diaminohexane hydrochloride ($n = 6$) recorded using MALDI IV with pulsed extraction.

decreasing intensity and the appearance of the spectrum is qualitatively reminiscent of a Flory distribution for a simple addition polymerization product. Under most recording conditions a set of peaks corresponding to simple oligomers detected as the proton, sodium cation and potassium cation adducts are observed but the spectrum in Fig. 12, which shows only the protonated series, was selected for the sake of clarity and simplicity of presentation. The major series of regularly spaced peaks, separated by the repeat unit mass of 170 amu, extends to 6460 amu, corresponding to a DP of 38. There is a second series of peaks which occurs at the oligomer mass minus 55 amu, which corresponds to the loss of the focal CH_2=CHCO unit, Fig. 13(1), or to one ion arising from a process of random amide link fragmentation, Fig. 13(2), which is consistent with the fact that fragmentation in polypeptides occurs at amide bonds. The absence of an ion corresponding to the other fragment expected from a random cleavage at amide links leads us to favour the first

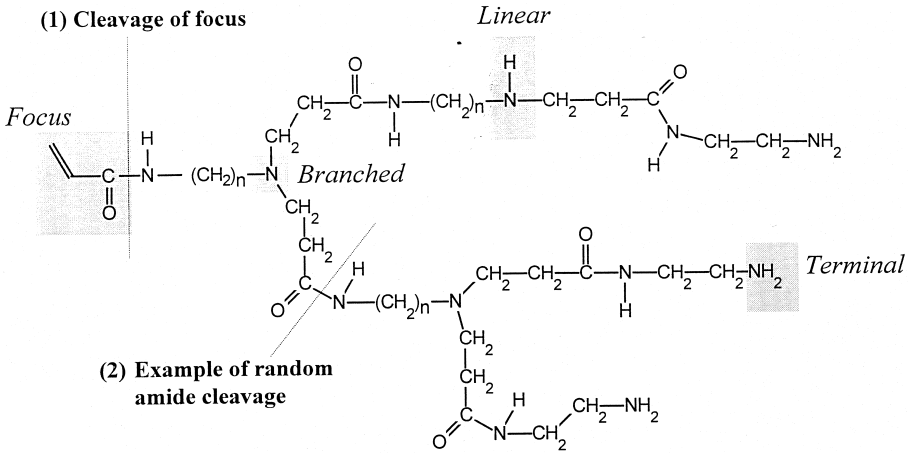

Fig. 13. Amide cleavage in a poly(amidoamine) hyperbranched system: (1) at focus; (2) random cleavage.

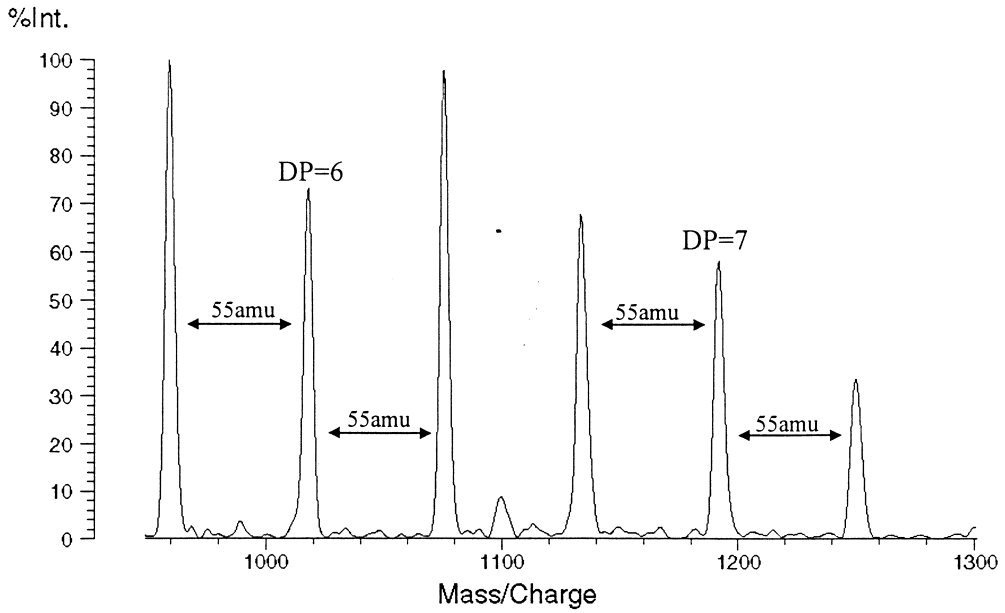

Fig. 14. MALDI-TOF mass spectrum (expansion 950–1300 *m*/*z*) of the polymer prepared from *N*-acryloyl-1,6-diaminohexane hydrochloride ($n = 6$) recorded using MALDI (IV), with dithranol as the matrix.

postulate. Considering the process of random amide fragmentation, depicted in Fig. 13(2), both of the fragments formed, namely at $M^+ - 55$ and $M^+ + 55$amu, would be expected to carry the attached charge equally well. Detection of these poly(amidoamine)s using the MALDI-TOF technique relies upon the fragments forming positively charged adducts of the corresponding free bases. As this positive charge is expected to be associated with the most basic group, in this case the free amine, it is assumed that both fragments resulting from a process of random amide cleavage would have a high probability of carrying a charge.

In further support of this view we observe that under conditions which favour fragmentation; namely a combination of matrix and sample solvents that do not allow good mixing and hence co crystallization (in this case an aqueous sample solution of polymer and dithranol in THF), both of the expected series of ions from random fragmentation at amide bonds can be seen; namely oligomer mass minus 55 amu and oligomer mass plus 55 amu. This is illustrated in the expanded section of a spectrum reproduced in Fig. 14. Also we observe that, under recording conditions which give the best signal to noise without excessive fragmentation, the comparative intensity of the minor series, at the oligomer masses minus 55 amu, Fig. 12, increases with increasing laser power, while for higher molecular weight samples of these polymers only the peaks for the oligomers minus the focus are detected. If the hyperbranched wedge can lose the A group at its focus then the possibility of termination of polymer growth by cyclization reactions in this system is very small and has to be discounted. Therefore we conclude that the poly(amidoamine) hydrochloride hyperbranched wedges retain their focal point and in this case intramolecular cyclization is not the dominant process, as for example is the case for many hyperbranched polyesters [25,27]. In our studies of AB_2 hyperbranched polyesters we have found that when cyclization occurs it occurs early in the reaction [33]. In the system under discussion here the cyclization process appears to be disfavoured as compared to propagation and growth. A possible rationalization for this preference is implied in Fig. 11, where association of the alkyl ammonium unit with the carbonyl oxygen is shown in preference to an association with the carbon–carbon double bond as required for cyclization. The conformational calculations also support the existence of this preference. We believe that such considerations provide a reasonable rationalization of the absence of any evidence for cyclization in this case.

The degree of branching of these poly(amidoamine) hyperbranched materials was determined using quantitative ^{15}N NMR spectroscopy. The ^{15}N NMR spectra, recorded at natural abundance in D_2O, were inverse-gated proton-decoupled to allow for quantitative comparison of integrated peak intensities; spectra were recorded at various relaxation delays from 10 to 120 s until no further variation in the spectra was observed.

Michael addition polymerization of these aminoacrylate monomers can, in principle, yield secondary or tertiary amines corresponding to linear or branched sub-units, Fig. 7. Thus amide and primary (terminal, T), secondary (linear, L) and tertiary (branched, B) amine nitrogen environments are possible, Fig. 15. The frequency of the branched and terminal groups is connected, $T = B + 1$. For polymers derived from *N*-acryloyl-α,ω-diaminoalkane hydrochlorides, each repeat unit contributes one amide and one amine nitrogen species. ^{15}N NMR spectroscopy revealed three signals for this system; the amide and primary

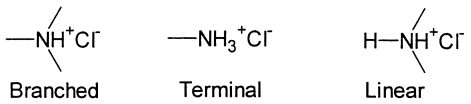

Fig. 15. Possible amine structural units.

amine nitrogens are readily identified on the basis of chemical shift (relative to liquid ammonia) and literature assignments of related compounds [34] but the signals for amine nitrogens in linear and branched units overlap; however, integration allows an assignment of the extent of branching.

Three signals are observed in all the spectra, which can be assigned as one amide and two amine salt signals. For polymers derived from *N*-acryloyl-1,2-diaminoethane hydrochloride, where $n = 2$, Fig. 16, the two amine salt signals are of approximately equal intensity and must represent terminal and branched units, since, if the polymer was composed entirely of linear units, the terminal contributions would be negligible (only one signal per chain) and the linear salt signal would be equal in intensity to the amide signal. In fact the sum of the relative intensities of the terminal and branched signals equals that of the amide signal within the limits of experimental error, an observation consistent with virtually complete branching. For this system the relationship between the degree of branching [14,15] and the terminal (T), branched (B) and amide (A) contributions can be expressed as: $DB = (B + T)/A$. The degree of experimental error associated with these calculations is such that the values obtained are the same no matter which definition for DB is favoured [14,15]. It can therefore be concluded that the polymer is highly branched with few or no linear units, within the limits of the experiment a degree of branching greater than 0.9 can be assigned. Therefore in the case where $n = 2$, we have a highly branched polymeric structure containing few or no linear sections, as illustrated in Fig. 17. It is proposed that steric hindrance within the polymer is overcome by allowing the terminal groups of shorter segments to be buried within the polymer structure, to give a system with perfect branching and irregular growth. Elemental analysis indicates an approximate composition of one HCl group for every polymer repeat unit; therefore all amine groups within the structure are represented as their hydrochloride salts, Fig. 17.

Table 1
Results from ^{15}N NMR spectroscopy experiments

Polymer $(CH_2)_n$	Amide salt signal (ppm)	Branched/linear amine signal (ppm)	Terminal amine signal (ppm)	DB
$n = 2$[a]	116.66	43.44	31.54	> 0.9
$n = 3$[b]	120.40	44.84	31.52	~0.65
$n = 4$[b]	125.24	45.48	33.32	~0.7
$n = 5$[b]	123.86	42.64	30.15	~0.65
$n = 6$[b]	125.14	43.59	31.65	~0.7
$n = 7$[b]	125.04	43.40	30.57	~0.65

[a]Recorded at pH ~1
[b]Recorded at pH ~3

Uniquely the monomer, *N*-acryloyl-1,2-diaminoethane hydrochloride ($n = 2$), gives such highly branched polymers; increasing the internal CH_2 chain length of the monomer was found to decrease the degree of branching. For example the polymers derived from *N*-acryloyl-1,4-diaminobutane ($n = 4$) display a branching factor of ~0.7, much closer to the statistical value proposed by Flory [13], Table 1. These conclusions are consistent with other spectroscopic characterization undertaken and supported by the results obtained from model reactions, see below.

No improvement in the resolution was observed if the spectra were acquired at 80°C. Solid state NMR techniques were examined in an attempt to gain an improved signal to noise ratio. The characterization of polymers derived from *N*-acryloyl-1,3-diaminopropane hydrochloride showed that quantitative analysis was not possible in the solid state; the resolution was poor and only two broad peaks were observed in the nitrogen spectrum, assigned as one amide and one amine salt signal.

2.4. Model reactions

A series of model reactions was undertaken in an attempt to gain a better understanding of the melt polymerization process. From Michael addition reactions between different ratios of [A:B] and [A:B_x] units we can conclude that the reaction in the melt is significantly more effective than the equivalent process carried out in solution. For example, the same products were obtained from the reaction of the B_6

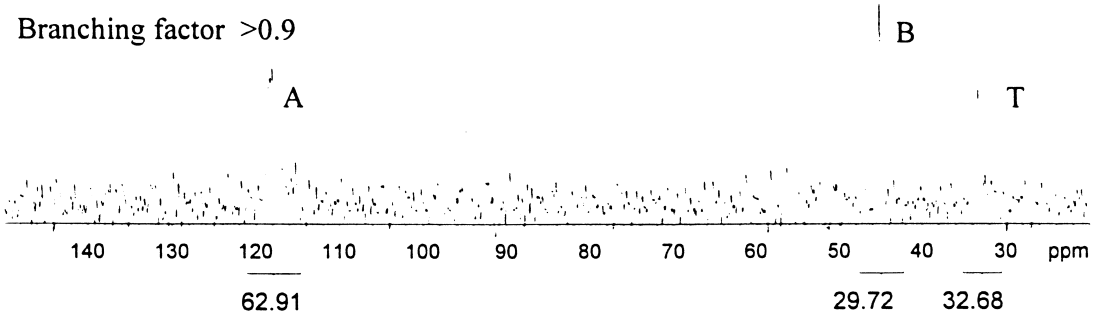

Fig. 16. Quantitative ^{15}N NMR spectra (D_2O); polymer prepared from *N*-acryloyl-1,2-diaminoethane hydrochloride (pH 1).

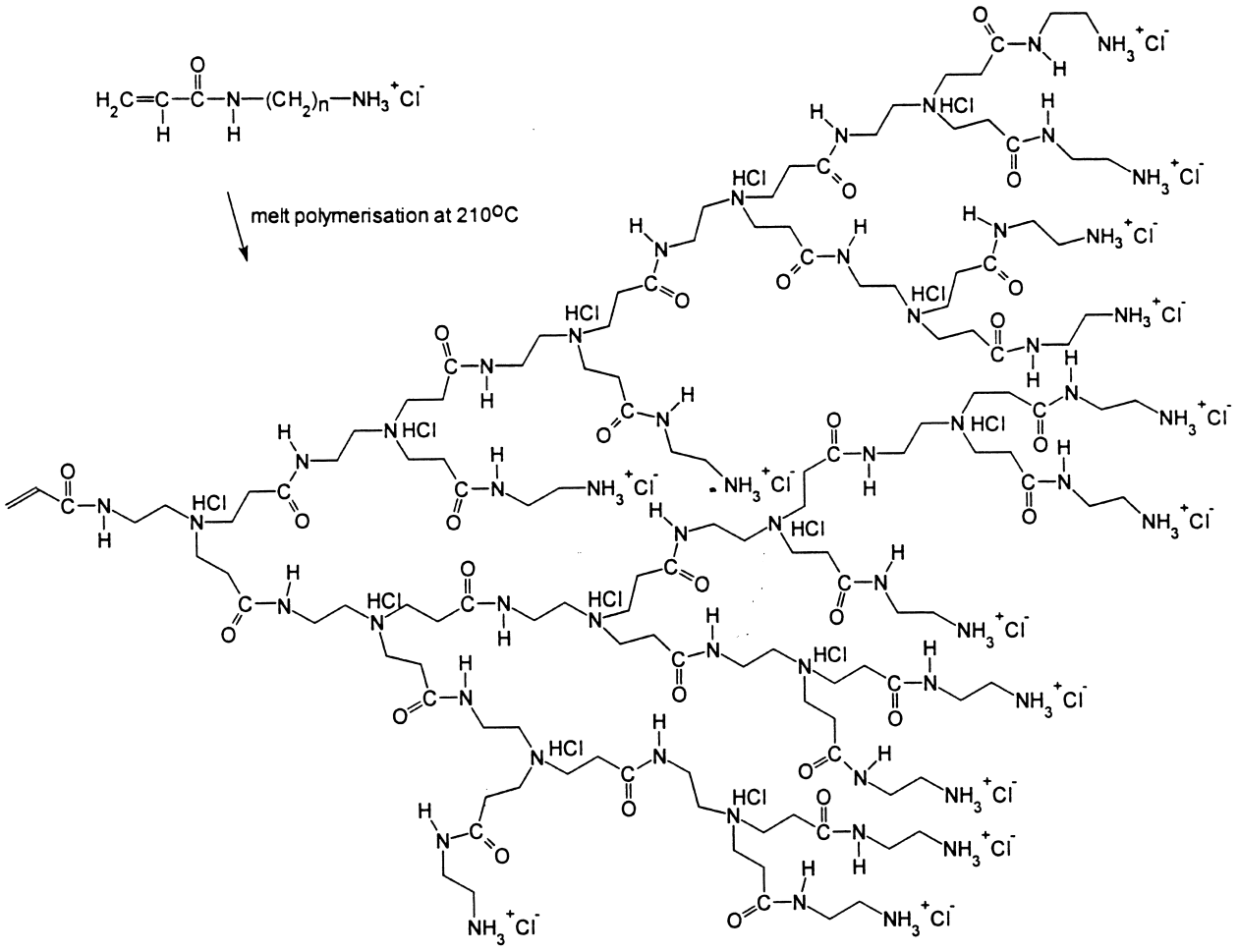

Fig. 17. Proposed structure of an AB_2 polymer hydrochloride salt.

unit, tris-(2-aminoethyl)amine, with six equivalents of the A unit, *N*-*t*-butoxycarbonyl-*N*′-acryloyl-1,2-diaminoethane, in methanol solution at 65°C for 216 h and a 4 h reaction in the melt at 160°C.

It appears to be assumed generally that the equimolar reaction between a primary amine and a Michael acceptor proceeds preferentially to give the 1:1 adduct. However, studies of model reactions indicate that a significant percentage of the reaction product is the 2:1 adduct. This is exemplified by the reaction between n-phenylacrylamide (X) and benzylamine (Y) at 160°C in the melt (Table 2).

2.5. Molecular weight comparisons

We have demonstrated how number average molecular weight information can be obtained from the ^{1}H NMR data, using end group counting techniques, Fig. 10. The method relies upon the premise that intramolecular cyclization between the focus and terminal amine units does not occur. MALDI-TOF mass spectrometry analysis shows that these hyperbranched wedges can lose the A group held at their focus, and thus the possible termination of polymer growth by cyclization reactions has to be discounted, allowing more reliability to be placed on the M_n values calculated from ^{1}H NMR data. Analysis of these poly(amidoamine) hydrochloride salts by MALDI-TOF mass spectrometry also provides data in support of the M_n values calculated from NMR spectroscopy, both techniques providing number average molecular weight information. There is a good correlation between the M_n results calculated from the MALDI-TOF spectra and those obtained from ^{1}H NMR spectroscopy for lower molecular weight samples only. Thus, analysis of the spectrum reproduced in Fig. 12 using the Kompact software gave a value of

Table 2
Results of model reactions

X:Y ratio	Analysis of reaction product ratios[a]	
	XY	X_2Y
1:1	1.65	1.0
2:1	1.0	10.0

[a]The ratios were established from the relative integrated intensities of the signals at 2.86 ppm [(Ph–NHCO**CH_2CH_2**)$_2$NCH_2–Ph], 3.00 ppm [(Ph–NHCO**CH_2CH_2**)NHCH_2–Ph] and 3.85 ppm [Ph–**CH_2NH_2**, (Ph–NHCO CH_2CH_2)NH**CH_2**–Ph)]

Table 3
Comparison of results calculated from ^{1}H NMR data and MALDI-TOF mass spectrometry

Sample ($n = 6$)	Data obtained from ^{1}H NMR spectra			Data obtained from MALDI-TOF[a]		
	DP_n	Extent of reaction (%)	α-value	α-value	DP_n[b]	r^2 [c]
1	9.2	89.17	0.446	0.323	2.8	0.99
2	12.8	92.15	0.461	0.360	3.6	0.93
3	41.4	97.58	0.488	0.354	3.4	0.73
4	46.9	97.87	0.490	0.297	2.5	0.97
5	62.4	98.40	0.492	0.160	1.5	0.95

[a]Assumes a Flory distribution[13]
[b]Calculated using the formula: number average DP = $1/(1 - \alpha(f - 1))$ where f = functionality (3 for an AB_2 system)
[c]Indicates how well the data fits, optimum being 1.0

1500 for M_n of the free base, compared with the value of 1570 calculated from the ^{1}H NMR spectrum. However, as we approach higher molecular weight, the MALDI-TOF spectra fail to provide a representative picture of the whole sample; the signal intensity from the high mass tail of the sample being insufficient to discriminate it from background noise and allow its incorporation into the analysis of the spectrum. It is also recognized that higher molecular weight species require higher laser power for the ionisation/desorption process than lower DP species [35]. So for AB_2 polymers with a wide polydispersity the distribution of oligomers observed will overestimate the proportion of low DP species in the sample. In line with this observation, attempts to fit the distributions obtained to the theoretical Flory distribution for non-linear polymers [13] using the expression

$$N_x = \frac{(fx - x)!}{(fx - 2x + 1)!x!}\alpha^{x-1}(1 - \alpha)^{(fx - 2x + 1)}$$

(where N_x = number of x-mer molecules, x = DP, f = functionality (3 for AB_2 systems) and α = fraction of B groups reacted) gave unrealistic α-values, Table 3. In these manual calculations all contributions to the spectrum from attached H^+, Na^+, K^+, P-55H^+, P-55Na^+ and P-55K^+ ion series were taken into consideration, circumventing the instrument software limitation which only deals with the main spectral series. The results, given in Table 3, show that although the data presented appear to fit the distribution well, the α-values calculated from the MALDI-TOF data are far too low, and too far removed from those calculated from the ^{1}H NMR spectra, to provide a sensible interpretation of the data.

Recent literature reports suggest that significant variations in the MALDI-TOF spectra observed for synthetic polymers of a broad polydispersity can be manipulated by doping the materials with different alkali metal cations [36], a narrowing of the polydispersity and an increase in molecular weight being observed with increasing cation size [37]. However, for this, and other AB_2 hyperbranched polymer systems studied, we report that detailed analysis reveals little change in the data collected as the size of the available cationic species is increased, although spectra generated with smaller attached cations were generally found to be better resolved. Progressing through the alkali metal series from lithium to caesium resulted in a decrease in the comparative intensity of the low DP species observed; however, it has been established that these oligomers are the most abundant species within the polymerization product at any reaction time, as predicted by Flory [13]. Therefore we conclude that, although it helps in the case of linear polymers, selective cation doping offers no help in improving the MALDI-TOF spectra of these hyperbranched systems and the phenomenon is specific rather than general.

2.6. Thermal analysis

The polymers have to be stored under dry nitrogen prior to analysis due to their extremely hygroscopic nature. Thermogravimetric analysis (Stanton Redcroft TG760 thermobalance, 5–10 mg, 10°C min^{-1}) indicated that dry polymers were thermally stable, all samples displaying less than 4% weight loss up to 300°C, after which extensive degradation and weight loss occurs. Differential scanning calorimetry (Perkin Elmer, DSC7 at 10°C min^{-1}) failed to reveal any crystalline melting points for any of these hyperbranched systems. This lack of crystallinity, due to disruption of packing by the branched segments, has been observed in a number of other hyperbranched and dendritic polymers [38,39]. Generally, hyperbranched polymers show a decrease in T_g in comparison with linear analogues. Although some problems concerning the reproducibility of data have been encountered, which may be due to plasticization of the samples by the absorption of water, a general trend of increasing T_g with increasing internal CH_2 chain length has been observed, with a pronounced odd/even effect, Fig. 18. The data recorded in Fig. 18 were measured using a set of samples prepared under standard conditions and on the same scale in the same apparatus (Table 4). The hygroscopic nature of these materials proved a problem in relation to elemental analysis and, although spectroscopic characterization and successful polymerization were indicative of pure monomers and precursors, elemental analysis gave slightly low values for percentage carbon in several cases (see experimental section). That the internal spacer chain length has an effect on T_g has been described for other AB_2 systems; increasing the

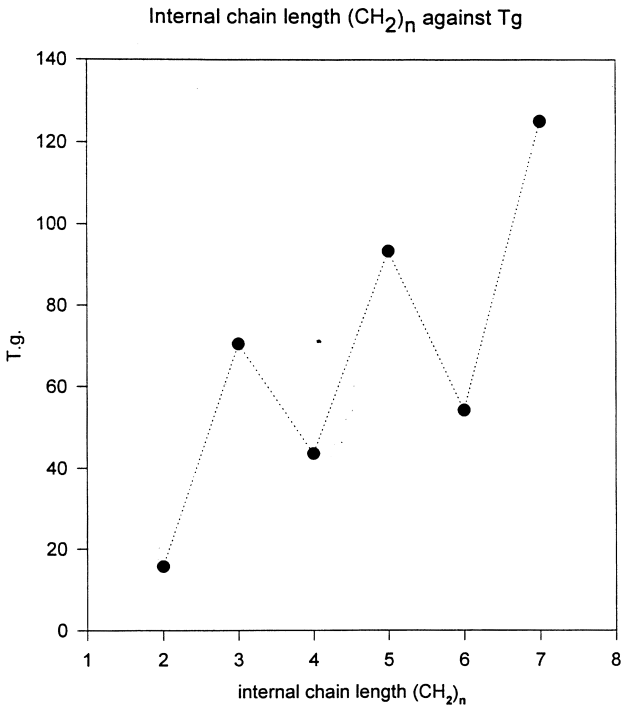

Fig. 18. Graph to show T_g as a function of internal CH_2 chain length for polymer samples prepared from *N*-acryloyl-α,ω-diaminoalkane hydrochlorides at 210°C for 4 h in the melt.

length of the oligoethyleneoxy spacer segments between the branch points has been shown to lower the T_g in hyperbranched polyurethanes [40] as does increasing the alkylene chain length for hyperbranched polyesters, derived from dimethyl-5-(hydroxyalkoxy)isophthalates [41]. The increase in T_g with increasing methylene spacer length in these systems is somewhat surprising and we have no explanation for it.

In our hands these hyperbranched polyelectrolytes were not amenable to analysis by aqueous gel permeation chromatography (GPC) as, even working at high ion concentration, the samples were absorbed directly onto the column. Similar results were observed by Voit and co-workers for the analysis of hyperbranched polyesters with terminal carboxylic acid functionalities [42].

Hyperbranched polymers have been shown to exhibit unusually low solution viscosity when compared to their linear analogues, which has been attributed to their molecular shape [43]. The poly(amidoamine) hydrochlorides reported here exhibit classic polyelectrolyte behaviour with respect to solution viscosity, which can be suppressed by the addition of 1% lithium chloride, Fig. 19. Extrapolation of the reduced viscosity, determined over a minimum of six different concentrations, to zero concentration gives an experimental value for intrinsic viscosity. Taking a series of readings for different molecular weight polymers (M_n, calculated by ^{1}H NMR spectroscopy, Table 5) the relationship between intrinsic viscosity and molecular weight can be established. Although it is more normal to consider M_w values for comparison with intrinsic viscosity measurements, a trend of decreasing viscosity with increasing M_n can be observed, a property closer to dendritic than linear behaviour; dendrimers with a similar structure show a viscosity maximum at approximately generation three, while linear systems follow the Mark Houwink equation displaying increasing intrinsic viscosity with molecular weight.

Table 4
Polymerization of $CH_2=CHCONH(CH_2)_nNH_3^+Cl^-$ on a 6 g scale at 210°C for 4 h

n	2	3	4	5	6	7
M_n[a]	17 400	4200	5800	9200	8500	15 900
DP[a]	116	26	63	48	41	72

[a]Measured by ^{1}H NMR spectroscopy

2.7. Core terminated AB_2/B_n copolymers

As their hydrochloride salts, these AB_2 poly (amidoamine) hyperbranched wedges are readily soluble in both water and methanol but are insoluble in water and all common organic solvents as their free bases. Further work has revealed that core terminated systems, prepared through AB_2/B_n copolymerizations using the AB_2 monomer *N*-acryloyl-1,2-diaminoethane hydrochloride, retain their solubility as free bases where the functionality of the core unit (B_n) ≥ 2. The monomer where $n = 2$ was selected for this study as not only in the standard AB_2 polymerization did it give the highest extent of reaction and a degree of branching approaching one, but in these AB_2/B_n copolymers it uniquely gave complete consumption of the acrylate group and therefore complete core termination of the polymer. Fig. 20 shows schematically how the addition of a small quantity of a B_3 core unit not only limits the molecular weight but also provides a single step route to pseudo-dendrimers. The observation that incorporation of a core terminating reagent has pronounced effects on the properties of the resultant materials is supported by the work of Hult et al. who reported marked solubility changes upon core termination of hyperbranched polyesters [44].

Standard AB_2 polymerization studies for this poly (amidoamine) hyperbranched system (see above) had established that variation of the polymethylene spacer length ($n = 2$–7) had a marked effect on both monomer reactivity and the structure (DB) and physical properties of the polymer; the monomer where $n = 2$ reacting much faster and achieving a higher degree of polymerisation than that where $n = 6$. This trend is reinforced in the AB_2/B_n copolymer studies, with materials prepared from the monomer where $n = 2$ exhibiting behaviour distinct from other samples. Core units of sufficiently high boiling point to remain in the reaction vessel and allow duplication of the reaction conditions used for the preparation of the standard AB_2 hyperbranched materials were selected. All reactions were carried out at 210°C under nitrogen for 4 h, after which there

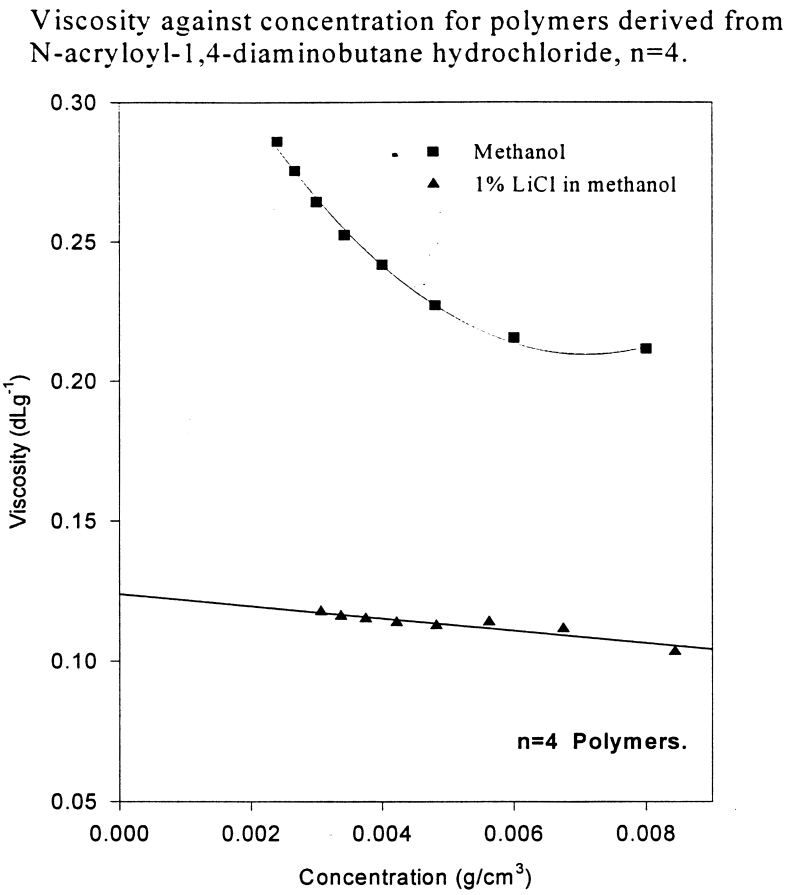

Fig. 19. Graph to show reduced viscosity against sample concentration for an AB_2 hyperbranched polymer where $n = 4$.

was no signal for the vinylic protons of the acrylamide functionality in the ^{1}H NMR spectrum of the product.

Hult and Malmström showed that the choice of B_n core units is critical in order to obtain a high degree of reaction of the core B groups in hyperbranched polyesters [45]; however, their discussion of the different core units is based on their comparative melt temperatures rather than their effects on the structure and properties of the resultant materials. We have carried out a series of AB_2/B_n copolymerizations using the monomer *N*-acryloyl-1,2-diaminoethane hydrochloride ($n = 2$) in conjunction with various B_n core terminators in order to investigate the effects of functionality and steric constraints in the core. B_n core units with amine groups (–NH and $–NH_2$) rather than the corresponding hydrochloride salts were selected as it was hoped that this would promote the preferential reactivity of the core units and hence complete core termination of the polymer. For this set of comparative polymerizations a core to monomer molar ratio of [1:100] was selected so that DB determined by quantitative ^{15}N NMR spectroscopy would, within the limits of the experiment, be unaffected by the signals due to the core. Where $n \geq 2$, only two nitrogen signals are observed in the spectrum, which we assigned as one amide (~114 ppm) and one amine (~30 ppm) salt signal (Fig. 21). The amine salt signal represents the terminal units as the shift observed, relative to liquid ammonia, is consistent with literature data for comparative structures [34]. The failure to detect any branched or linear amine salt signals parallels the observations of Meijer et al. on poly(propyleneimine) dendrimers [34], presumably the multiplicity of environments and broadness of the lines 'smears out' the signals to make them indistinguishable from the noise. As the frequency of occurrence of the terminal and branched groups is connected, Terminal = (Branched + 1), the equation [14] DB = (Branched + Terminal)/Amide can be used to estimate the extent of branching.

Table 5
Intrinsic viscosity data for polymer hydrochloride salts, where $n = 4$

M_n (by ^{1}H NMR)	Extent of reaction (%)	Intrinsic viscosity (η)[a] (ml g^{-1})
4940	96.4	1.76
5800	97.0	1.56
6140	97.1	1.74
7600	97.7	1.23
6470	97.3	1.36
8500	97.9	1.26
11 900	98.4	1.24

[a]1% LiCl in methanol at 25°C

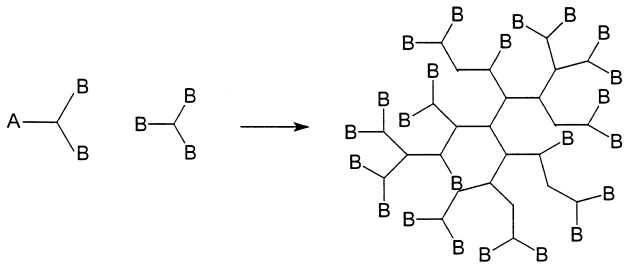

Fig. 20. Hypothetical AB_2/B_3 copolymer.

From the accumulated data, Table 6, we can conclude that the structure and degree of flexibility of the core are factors influencing the extent of branching. The branching factors calculated for these AB_2/B_n copolymers appear to be related to the minimum energy conformations modelled for these core units. This is illustrated by comparison of the predicted conformations of 1,4,7-triazacyclononane (B_3), 1,5,9-triazacyclododecane (B_3) and tris-(2-aminoethylamine) (B_6), a markedly higher degree of branching being observed for the flexible sterically accessible B_6 core terminator as compared to the two more sterically constrained B_3 molecules, Table 5 and Fig. 22. Modification of the core to monomer ratio allows a degree of control over the molecular weight of the resultant materials [46]. Core to monomer ratios appropriate for the synthesis of successive generations of idealized dendrimers were calculated for synthesis of core terminated polymers using the B_6 core.

Degree of branching has been shown to be a poor indication of topology, Figs 3 and 4, but a reasonable test of dendritic character lies in the direct comparison of the solution behaviour of these AB_2/B_6 copolymers with their perfectly regular mono-disperse dendrimer analogues. Solution viscosity measurements on the resultant polyelectrolytes were carried out in 1% aqueous lithium chloride solution at 25°C over a range of dilutions, using a Laude/Schott automated system. A plot of reduced viscosity against concentration allows extrapolation to zero concentration to give a value for intrinsic viscosity ($cm^3\ g^{-1}$), see Table 7.

The logs of the observed intrinsic viscosities were plotted against the logs of molecular weights calculated from the monomer to core terminator ratios and are shown in Fig. 23 in comparison with published data for Tomalia's PAMAM dendrimers [47]. These results are in line with those previously reported for the AB_2 poly(amidoamine) hyperbranched materials where at high degrees of conversion, a trend of decreasing intrinsic viscosity with increasing molecular weight is observed [17,18], Table 5.

We do not expect that this simple 'one-pot' synthesis will produce perfect monodisperse dendrimers, indeed a distribution in both molecular weight and structure is to be expected. However, it is clear that in the system examined the peak in the graph of log of intrinsic viscosity versus molecular weight is demonstrated and is consistent with the formation of polymeric materials with topologies giving rise to solution viscosity behaviour resembling that of dendrimers [48].

3. Conclusions

In summary, we have established a simple 'one-pot' route to the hyperbranched hydrochloride salt analogues of the Tomalia PAMAM dendrimers and related structures and demonstrated that examples of these materials exhibit a high degree of branching and some of the solution properties of perfectly regular dendrimers. Addition of a core terminating unit has been shown to affect solubility and facilitate control over both molecular weight and degree of branching. Dendritic solution viscosity behaviour has been demonstrated in core terminated hyperbranched poly (amidoamines).

Work in progress, modifying the hyperbranched poly (amidoamines) reported here to improve their physical properties, indicates that polymerization of methacryloyl-α,ω-diaminoalkane derivatives gives materials which have more favourable solubility behaviour than their acrylate analogues. This work will be the subject of further reports.

4. Experimental

All chemicals were purchased from either Lancaster Synthesis or Aldrich Chemical Company and used as received without further purification.

4.1. Instrumentation

Infrared spectra were recorded as thin films on NaCl plates, unless otherwise stated, using a Perkin Elmer 1600

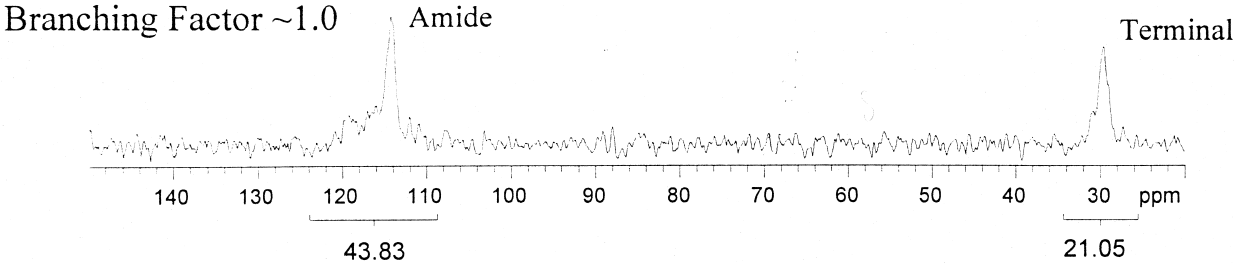

Fig. 21. Quantitative ^{15}N NMR spectra (D_2O); copolymer prepared from *N*-acryloyl-1,2-diaminoethane hydrochloride and tris-(2-aminoethylamine).

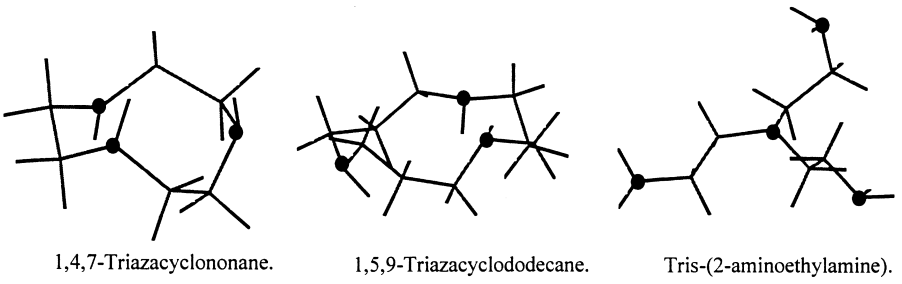

Fig. 22. Predicted minimum energy conformations for B_3 and B_6 core units (Biosym), where ● represents the amine nitrogen.

series spectrometer. ^{1}H, ^{13}C and ^{15}N NMR spectra were recorded using a Varian 400 MHz NMR spectrometer. MALDI-TOF mass spectra were recorded using a Kratos Kompact MALDI IV instrument operated in linear detection mode to generate positive ion spectra unless otherwise stated. Samples (2 mg ml^{-1}, water) were using 2,5-dihydroxybenzoic acid (10 mg ml^{-1} [40:60] water/acetonitrile) as the matrix and the spectra obtained calibrated externally. Viscosity measurements were carried out at 25°C over a range of dilutions, using a Laude/Schott automated system. Elemental analyses were obtained using a Carlo-Erba instrument, some of the intermediates were marginally low on carbon probably due to the problem of water absorption in these hygroscopic materials.

4.2. Monomer synthesis

The monomer synthesis involved three steps. As an example, the detailed procedure is given for the synthesis of *N*-acryloyl-1,2-diaminoethane hydrochloride, from 1,2-diaminoethane via *N*-*t*-butoxycarbonyl-1,2-diaminoethane and *N*-*t*-butoxycarbonyl-*N*′-acryloyl-1,2-diaminoethane. Only yields and characterization data are recorded for the other five monomers which were produced in a completely analogous manner, except for the precursor N-*t*-butoxycarbonyl-1,6-diaminohexane where the literature method [15] was used.

4.2.1. Step 1(a)

4.2.1.1. N-t-Butoxycarbonyl-1,2-diaminoethane. To a 2 l flange flask cooled in an ice/salt bath (−10 to 0°C) fitted with a condenser, pressure equalising dropping funnel, mechanical stirrer and nitrogen inlet was added a solution of ethylenediamine (45 g, 733 mM) in dichloromethane (400 ml). A solution of BOC-anhydride (40 g, 183 mM) in dichloromethane (200 ml) was added dropwise over 2 h with stirring. The mixture was allowed to warm to room temperature and stirred overnight (16 h). The solvent was removed by rotary evaporation and addition of water (200 ml) resulted in the precipitation of a white solid which was identified as *N*,*N*′-(bis-*t*-butoxycarbonyl)-1,2-diaminoethane (1.4 g, 5.38 mM) by IR, ^{1}H NMR and ^{13}C NMR spectroscopy which was in agreement with the reported literature data. IR at λ_{max} (KBr disc): 3377, 2988, 2936, 1682, 1527, 1446, 1393, 1368, 1279, 1240, 1164, 983,

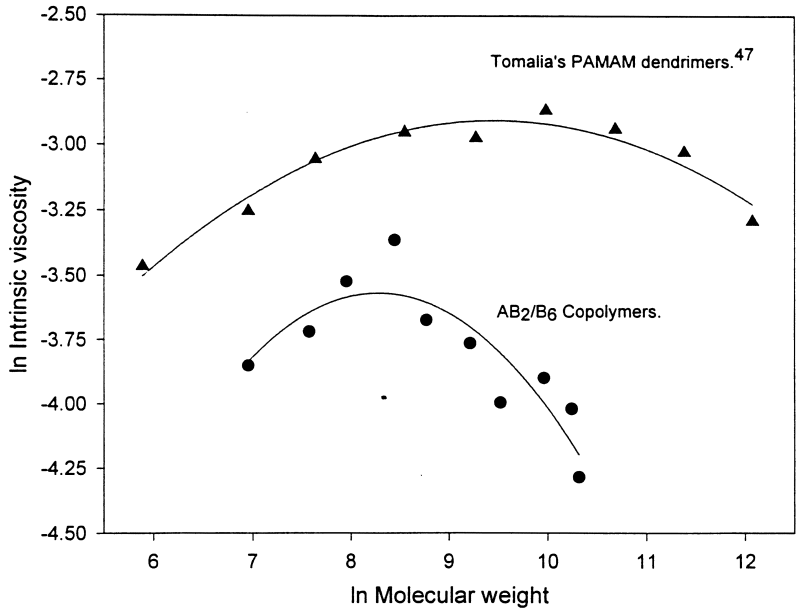

Fig. 23. Molecular weight/intrinsic viscosity relationship for AB_2/B_6 copolymers.

Table 6
Copolymerization of *N*-acryloyl-1,2-diaminoethane hydrochloride with different B_n core terminators

B_n	Core	M.p. (°C)	Amide (ppm)	Amine (ppm)	[C:M]	DB
B_6	Tris-(2-aminoethylamine)	< 25	114.0	29.6	1:100	~1.0
B_4	*p*-Xylylenediamine	62–64	114.1	29.1	1:100	~0.9
B_3	1,4,7-Triazacyclononane	43–45	114.5	30.8	1:100	~0.4
B_3	1,5,9-Triazacyclododecane	33–36	114.2	28.8	1:100	~0.6
B_2	1-Decylamine	12–14	114.0	29.0	1:100	~0.9
B_1	*N,N′*-Dioctylamine	14–15	116.1	43.4, 31.6	1:100	~1.0

872, 783, 611 cm^{-1}. ^1H NMR ($CDCl_3$): $\delta = 1.44$ (s, 18H, CH_3); 3.23 (m, 4H, CH_2); 4.86 (bs, 2H, amide protons). ^{13}C NMR ($CDCl_3$): $\delta = 28.36, 40.80, 79.44, 150.99$.

The filtrate was saturated with sodium chloride, extracted with ethyl acetate (3 × 100 ml) and the combined organic fractions concentrated under reduced pressure to give a pale oil. Residual sodium chloride was removed by dissolving the oil in chloroform (100 ml) and filtering through a porosity 3 sinter. The solvent was removed under reduced pressure and the product dried under vacuum to yield *N-t*-butoxycarbonyl-1,2-diaminoethane (27.2 g, 170 mM, 93%) as a colourless oil. Calculated for $C_7H_{16}N_2O_2$: C, 52.50; H, 10.00; N, 17.50%; found: C, 52.58; H, 9.79; N, 17.34%. IR at λ_{max}: 3360, 2976, 2932, 2869, 1694, 1525, 1365, 1173 cm^{-1}. ^1H NMR ($CDCl_3$): $\delta = 1.28$ (m, 2H, NH_2); 1.45 (s, 9H, CH_3); 2.80 (m, 2H, CH_2); 3.18 (m, 2H, CH_2); 5.04 (bs, 1H, amide proton). ^{13}C NMR ($CDCl_3$): $\delta = 28.33$, 41.80, 43.33, 79.09, 156.16. The signals in the ^1H NMR spectrum at $\delta = 1.28$ and 5.04 due to NH_2 and amide protons disappeared on shaking with D_2O.

4.2.1.2. N-t-Butoxycarbonyl-1,3-diaminopropane (89%). Calculated for $C_8H_{18}N_2O_2$: C, 55.17; H, 10.34; N, 16.09%; found: C, 52.66; H, 11.02; N, 15.37%. IR at λ_{max}: 3359, 2975, 2932, 2867, 1696, 1526, 1365, 1275, 1252, 1174 cm^{-1}. ^1H NMR ($CDCl_3$): $\delta = 1.27$ (m, 2H, NH_2); 1.44 (s, 9H, CH_3); 1.61 (m, 2H, CH_2); 2.76 (m, 2H, CH_2); 3.21 (m, 2H, CH_2); 4.94 (m, 1H, amide proton). ^{13}C NMR ($CDCl_3$): $\delta = 28.38, 33.40, 38.40, 39.62, 79.01$, 156.09. The signals in the ^1H NMR spectrum at $\delta = 1.27$ and 4.94 due to NH_2 and amide protons disappeared on shaking with D_2O.

4.2.1.3. N-t-Butoxycarbonyl-1,4-diaminobutane (93%). Calculated for $C_9H_{20}N_2O_2$: C, 57.45; H, 10.64; N, 14.89%; found: C, 55.07; H, 10.47; N, 14.67%. IR at λ_{max}: 3356, 2975, 2932, 2865, 1695, 1527, 1454, 1391, 1365, 1275, 1251, 1174 cm^{-1}. ^1H NMR ($CDCl_3$): $\delta = 1.28$ (m, 2H, NH_2); 1.44 (s, 9H, CH_3); 1.40–1.54 (m, 4H, CH_2); 2.71 (m, 2H, CH_2); 3.13 (m, 2H, CH_2); 4.66 (bs, 1H, amide proton). ^{13}C NMR ($CDCl_3$): $\delta = 26.89, 27.89, 30.25$, 39.77, 41.17, 78.02, 155.63. The signals in the ^1H NMR spectrum at $\delta = 1.28$ and 4.66 due to NH_2 and amide protons disappeared on shaking with D_2O.

4.2.1.4. N-t-Butoxycarbonyl-1,5-diaminopentane (92%). Calculated for $C_{10}H_{22}N_2O_2$: C, 59.41; H, 10.89; N, 13.86%; found: C, 57.63; H,10.59; N, 13.21%. IR at λ_{max}: 3360, 2974, 2930, 2858, 1698, 1529, 1365, 1275, 1251, 1174 cm^{-1}. ^1H NMR ($CDCl_3$): $\delta = 1.24$ (m, 2H, NH_2); 1.35 (m, 2H, CH_2); 1.44 (s, 9H, CH_3) 2.69 (m, 2H, CH_2); 3.12 (m, 2H, CH_2); 4.58 (bs, 1H, amide proton). ^{13}C NMR ($CDCl_3$): $\delta = 24.05, 28.40, 29.93, 33.41, 40.50, 42.08$, 79.00, 155.96. The signals in the ^1H NMR spectrum at $\delta = 1.24$ and 4.58 due to NH_2 and amide protons disappeared on shaking with D_2O.

4.2.1.5. N-t-Butoxycarbonyl-1,7-diaminoheptane (88%). Calculated for $C_{12}H_{26}N_2O_2$: C, 62.61; H, 11.30; N,

Table 7
Copolymerization of *N*-acryloyl-1,2-diaminoethane hydrochloride ($n = 2$) and tris-(2-aminoethylamine) (B_6 core)

C:M molar ratio	Theoretical generation	Theoretical molecular weight	Intrinsic viscosity (η)[a] (ml g^{-1})
1:6	1	1046	2.13
1:12	(1.5)	1946	2.42
1:18	2	2846	2.94
1:30	(2.5)	4646	3.46
1:42	3	6446	2.53
1:66	(3.5)	10 046	2.31
1:90	4	13 646	1.83
1:138	(4.5)	20 846	2.02
1:186	5	28 046	1.79[b]
1:282	(5.5)	42 446	2.16[b]
1:378	6	56 846	2.05[b]

[a]1% LiCl in water at 25°C
[b]Substantial errors as < 26 mg of core unit required to be polymerized with 5 g of monomer; errors due to both weighing and mixing in the reactor

12.17%; found: C, 59.16; H, 10.49; N, 10.97%. IR at λ_{max}: 3356, 2975, 2928, 2855, 1696, 1528, 1454, 1390, 1365, 1251, 1174 cm^{-1}. ^1H NMR ($CDCl_3$): $\delta = 1.31$ (m, 10H, CH_2); 1.45 (s, 9H, CH_3); 1.62 (m, 2H, NH_2); 2.68 (m, 2H, CH_2); 3.10 (m, 2H, CH_2); 4.61 (bs, 1H, amide proton). ^{13}C NMR ($CDCl_3$): $\delta = 26.70, 26.73, 28.37, 29.06, 29.95, 33.62, 40.51, 42.09, 78.93, 155.95$.

4.2.2. Step 1(b)

4.2.2.1. N-t-Butoxycarbonyl-1,6-diaminohexane. To a three-necked round bottomed flask fitted with a magnetic stirrer, condenser, pressure equilibrating dropping funnel and nitrogen inlet, containing a stirred solution of 1,6-diaminohexane (40 g, 344 mM) in dioxan (120 ml) was added a solution of s-*t*-butoxycarbonyl-4,6-dimethyl-2-mercaptopyrimidine (25 g, 104 mM) in dioxan (100 ml) dropwise over 3 h. The reaction mixture was stirred at room temperature for 16 h. The precipitated 4,6-dimethyl-2-mercaptopyrimidine was removed from solution by filtration and the filtrate concentrated to 100 ml. The addition of water (200 ml) to the solution afforded a white precipitate, which was isolated by filtration, washed with diethyl ether and dried under vacuum to give bis-(*N*,*N*′-*t*-butoxycarbonyl)-1,6-diaminohexane [11] (3.62 g, 9.628 mM, 18.5%). Calculated for $C_{16}H_{32}O_4N_2$: C, 60.76; H, 10.13; N, 8.86%; found: C, 60.18; H, 10.11; N, 9.08%. IR at λ_{max} (KBr disc): 3373, 2983, 2940, 2873, 1688, 1521, 1365, 1276, 1266, 1251, 1174, 1049, 977, 871, 780, 601 cm^{-1}. ^1H NMR ($CDCl_3$): $\delta = 1.32$ (m, 4H, CH_2); 1.44 (s, 18H, CH_3); 1.47 (m, 2H, CH_2); 1.75 (m, 2H, CH_2); 3.10 (m, 4H, CH_2); 4.57 (bs, 2H, amide proton). ^{13}C NMR ($CDCl_3$): $\delta =$ 26.30, 28.39, 29.94, 40.34, 79.04, 155.99.

Dioxan was removed from the filtrate under reduced pressure and the aqueous solution saturated with sodium chloride (50 g) and extracted with ethyl acetate (3 × 100 ml). The combined organic fractions were concentrated under reduced pressure and redissolved in water (150 ml). The resultant aqueous solution was acidified to pH 3 with hydrochloric acid and extracted with ethyl acetate. Saturation of the aqueous solution with sodium chloride afforded a white precipitate, which was isolated by filtration, washed with diethyl ether and dried under vacuum to afford *N-t-* butoxycarbonyl-1,6-diaminohexane hydrochloride [11] (21.22 g, 84.2 mM, 81%, m.p. 163°C, lit. m.p. [11] 162.5–163°C). Calculated for $C_{11}H_{25}O_2N_2Cl$: C, 52.38; H, 9.92; N, 11.11%; found: C, 52.34; H, 10.15; N, 11.07%. IR at λ_{max} (KBr disc): 3374, 2935, 1693, 1610, 1524, 1173 cm^{-1}. ^1H NMR (D_2O): $\delta = 1.24$ (m, 2H, CH_2); 1.30 (bs, 9H, CH_3); 1.36 (m, 2H, CH_2); 1.54 (m, 2H, CH_2); 2.86 (m, 2H, CH_2); 2.93 (m, 2H, CH_2). ^{13}C NMR (D_2O): $\delta =$ 25.00, 25.13, 26.41, 27.50, 28.45, 39.23, 39.59, 80.61, 171.78.

A solution of *N-t*-butoxycarbonyl-1,6-diaminohexane hydrochloride (34 g, 134.9 mM) in water (150 ml) was basified to pH 14 by the dropwise addition of a concentrated sodium hydroxide solution. After 10 min the solution was extracted with chloroform (2 × 100 ml) and the combined organic fractions concentrated under reduced pressure. Drying under vacuum afforded a pale oil, *N-t*-butoxycarbonyl-1,6-diaminohexane [11] (28.3 g, 131.0 mM, 97%). ^1H NMR ($CDCl_3$): $\delta = 1.28$ (s, 2H, NH_2); 1.35 (m, 6H, CH_2); 1.45 (m, 9H, CH_3); 1.50 (m, 2H, CH_2); 2.69 (m, 2H, CH_2); 3.12 (m, 2H, CH_2); 4.62 (bs, 1H, amide proton). ^{13}C NMR ($CDCl_3$): $\delta = 26.49, 28.37, 30.00, 33.67, 40.44, 42.07, 78.92, 155.93$.

4.2.3. Step 2

4.2.3.1. N-t-Butoxycarbonyl-N′-acryloyl-1,2-diaminoethane. To a well-stirred solution of acryloyl chloride (13.6 g, 0.150 mol) in chloroform (300 ml) cooled in an ice/salt bath (− 10 to 0°C) was added a solution of triethylamine (12.65 ml, 0.125 mol) and *N-t*-butoxycarbonyl-1,2-diaminoethane (20 g, 0.125 mol) in chloroform (150 ml) dropwise over 1 h. After addition, the reaction was allowed to equilibrate to room temperature and stirred for 1 h before the solvent was removed under reduced pressure. The residue was washed with water and extracted with chloroform (3 × 150 ml). The combined organic fractions were concentrated under reduced pressure and the resultant white solid dried under vacuum to give *N-t*-butoxycarbonyl-*N′*- acryloyl-1,2-diaminoethane (23.7 g, 110 mM, 89%, m.p. 102.6–103°C). Calculated for $C_{10}H_{18}N_2O_3$: C, 56.07; H, 8.41; N, 13.08%; found: C, 55.63; H, 8.48; N, 13.30%. IR at λ_{max}: 3454, 3331, 3006, 2981, 2935, 1697, 1662, 1627, 1518, 1367, 1250, 1169, 976 cm^{-1}. ^1H NMR ($CDCl_3$): $\delta =$ 1.44 (s, 9H, CH_3); 3.33 (m, 2H, CH_2); 3.44 (m, 2H, CH_2); 5.05 (bs, 1H, amide proton); 5.63 (m, 1H, vinyl proton); 6.10 (m, 1H, vinyl proton); 6.26 (m, 1H, vinyl proton); 5.65 (bs, 1H, amide proton). ^{13}C NMR ($CDCl_3$): $\delta =$ 28.32, 40.05, 41.00, 79.78, 126.23, 130.85, 157.11, 166.19.

4.2.3.2. N-t-Butoxycarbonyl-N′-acryloyl-1,3-diaminopropane (80%, m.p. above decomposition temperature). Calculated for $C_{11}H_{20}N_2O_3$: C, 57.89; H, 8.77; N, 12.28%; found: C, 57.27; H, 8.99; N, 12.12%. IR at λ_{max}: 3317, 2980, 2935, 1694, 1660, 1625, 1530, 1367, 1251, 1171, 983, 957, 863 cm^{-1}. ^1H NMR ($CDCl_3$): $\delta = 1.44$ (s, 9H, CH_3); 1.65 (m, 2H, CH_2); 3.19 (m, 2H, CH_2); 3.38 (m, 2H, CH_2); 5.04 (bs, 1H, amide proton); 5.64 (m, 1H, vinyl proton); 6.22 (m, 2H, vinyl proton); 6.66 (bs, 1H, amide proton). ^{13}C NMR ($CDCl_3$): $\delta = 28.35, 30.10, 35.77, 36.97, 79.37, 126.04, 131.07, 158.43, 165.88$.

4.2.3.3. N-t-Butoxycarbonyl-N′-acryloyl-1,4-diaminobutane (81%, m.p. 103.5–104°C). Calculated for $C_{12}H_{22}N_2O_3$: C, 59.50; H, 9.09; N, 11.57; found: C, 59.11; H, 9.20; N, 11.13%. IR at λ_{max}: 3453, 3329, 3016, 1700, 1665, 1513,

1367, 1216, 1169, 771 cm^{-1}. ^1H NMR ($CDCl_3$): $\delta = 1.44$ (s, 9H, CH_3); 1.56 (m, 4H, CH_2); 3.14 (m, 2H, CH_2); 3.35 (m, 2H, CH_2); 4.71 (bs, 1H, amide proton); 5.63 (m, 1H, vinyl proton); 6.15 (m, 2H, vinyl protons); 6.22 (bs, 1H, amide proton). ^{13}C NMR ($CDCl_3$): $\delta = 26.43, 27.70, 28.37, 39.16, 39.98, 79.22, 126.13, 130.90, 156.16, 165.64$.

4.2.3.4. N-t-Butoxycarbonyl-N′-acryloyl-1,5-diaminopentane (76%, m.p. 71.5–72°C). Calculated for $C_{13}H_{24}N_2O_3$: C, 60.94; H, 9.38; N, 10.94%; found: C, 60.77; H, 9.59; N, 10.98%. IR at λ_{max}: 3306, 2980, 2935, 2856, 1688, 1662, 1626, 1535, 1480, 1411, 1368, 1320, 1270, 1249, 1176, 992, 959, 706, 648 cm^{-1}. ^1H NMR ($CDCl_3$): $\delta = 1.36$ (m, 2H, CH_2); 1.44 (s, 9H, CH_3); 1.51 (m, 2H, CH_2); 1.57 (m, 2H, CH_2); 3.11 (m, 2H, CH_2); 3.33 (m, 2H, CH_2); 4.62 (bs, 1H, amide proton); 5.62 (m, 1H, vinyl proton); 5.09 (bs, 1H, amide proton); 6.11 (m, 1H, vinyl proton); 6.28 (m, 1H, vinyl proton). ^{13}C NMR ($CDCl_3$): $\delta = 23.86, 28.40, 29.01, 29.72, 39.32, 40.13, 79.10, 126.17, 130.89, 156.13, 165.59$.

4.2.3.5. N-t-Butoxycarbonyl-N′-acryloyl-1,6-diaminohexane[15] (85%, m.p. 108–108.5°C, lit. m.p.[11] 108.5–109.5°C). Calculated for $C_{14}H_{26}O_3N_2$: C, 62.22; H, 9.63; N, 10.37%; found: C, 61.68; H, 9.89; N, 10.37%. IR at λ_{max}: 3329, 2934, 1650, 1605, 1538, 1505, 1477, 1458, 1320, 1210, 1158, 925, 870, 790, 730, 641 cm^{-1}. ^1H NMR ($CDCl_3$): $\delta = 1.31$ (m, 4H, CH_2), 1.42 (m, 9H, CH_3), 1.46 (m, 2H, CH_2), 1.49 (m, 2H, CH_2), 2.19 (bs, 1H, amide proton), 3.07 (m, 2H, CH_2), 3.28 (m, 2H, CH_2), 4.66 (bs, 1H, amide proton), 5.58 (d, 1H, vinyl proton), 6.10 (m, 2H, vinyl protons). ^{13}C NMR ($CDCl_3$): $\delta = 25.88, 26.05, 28.35, 29.23, 29.91, 39.04, 40.02, 78.99, 125.93, 131.00, 156.10, 165.59$

4.2.3.6. N-t-Butoxycarbonyl-N′-acryloyl-1,7-diaminoheptane (92%). Calculated for $C_{15}H_{28}N_2O_3$: C, 63.38; H, 9.86; N, 9.86%; found: C, 62.36; H, 9.92; N, 10.47%. IR at λ_{max}: 3358, 2974, 2928, 2855, 1698, 1528, 1454, 1390, 1365, 1274, 1251, 1174, 1041, 870, 754 cm^{-1}. ^1H NMR ($CDCl_3$): $\delta = 1.33$ (m, 8H, CH_2); 1.44 (s, 9H, CH_3); 1.53 (m, 2H, CH_2); 3.10 (m, 2H, CH_2); 3.33 (m, 2H, CH_2); 4.59 (bs, 1H, amide proton); 5.62 (m, 1H, vinyl proton); 5.79 (bs, 1H, amide proton); 6.12 (m, 1H vinyl proton); 6.25 (m, 1H, vinyl proton). ^{13}C NMR ($CDCl_3$): $\delta = 26.52, 26.71, 28.40, 28.74, 29.39, 29.88, 39.46, 40.42, 79.01, 126.17, 130.92, 155.98, 165.49$.

4.2.4. Step 3

4.2.4.1. N-Acryloyl-1,2-diaminoethane hydrochloride. A stirred solution of *N-t*-butoxycarbonyl-*N′*-acryloyl-1,2-diaminoethane (10.11 g, 47.2 mM) in ethyl acetate (100 ml) was acidified to pH 1 by the dropwise addition of concentrated hydrochloric acid. After 30 min at room temperature the solvent was removed under reduced pressure and the residue triturated with diethyl ether and dried under vacuum to afford *N*-acryloyl-1,2-diaminoethane hydrochloride (6.32 g, 42.1 mM, 89%). IR at λ_{max}: 3396, 3062, 1657, 1620, 1550, 1325, 1250, 1169, 979, 804 cm^{-1}. ^1H NMR (D_2O): $\delta = 3.05$ (m, 2H, CH_2); 3.44 (m, 2H, CH_2); 5.65 (m, 1H, vinyl proton); 6.10 (m, 2H, vinyl protons). ^{13}C NMR (D_2O): $\delta = 36.63$; 39.03, 127.86, 129.38, 169.21.

4.2.4.2. N-Acryloyl-1,3-diaminopropane hydrochloride (95%). IR at λ_{max}: 3268, 2965, 1658, 1624, 1548, 1408.5, 1367, 1251, 1167, 1066, 986, 806, 668 cm^{-1}. ^1H NMR (D_2O): $\delta = 1.77$ (m, 2H, CH_2); 2.88 (m, 2H, CH_2); 3.23 (m, 2H, CH_2); 5.62 (m, 1H, vinyl proton); 6.07 (m, 2H, vinyl proton). ^{13}C NMR ($CDCl_3$): $\delta = 26.45, 35.90, 36.85, 127.30, 129.56, 168.69$.

4.2.4.3. N-Acryloyl-1,4-diaminobutane hydrochloride (97%). IR at λ_{max}: 3258, 2939, 1650, 1614, 1556, 1512, 1482, 1410, 1241, 1168, 1059, 987, 967, 808, 691, 534 cm^{-1}. ^1H NMR (D_2O): $\delta = 1.42$ (m, 4H, CH_2); 2.78 (m, 2H, CH_2); 3.07 (m, 2H, CH_2); 5.51 (m, 1H, vinyl proton); 5.99 (m, 2H, vinyl protons). ^{13}C NMR (D_2O): $\delta = 23.92, 25.16, 38.39, 38.88, 126.98, 129.70, 168.30$.

4.2.4.4. N-Acryloyl-1,5-diaminopentane hydrochloride (95%). IR at λ_{max}: 3239, 2933, 1688, 1626, 1551, 1468, 1409, 1372, 1314, 1246, 1140, 1071, 980, 719 cm^{-1}. ^1H NMR (D_2O): $\delta = 1.23$ (m, 2H, CH_2); 1.40 (m, 2H, CH_2); 1.50 (m, 2H, CH_2); 2.81 (m, 2H, CH_2); 3.10 (m, 2H, CH_2); 5.57 (m, 1H, vinyl proton); 6.04 (m, 2H, vinyl protons). ^{13}C NMR (D_2O): $\delta = 22.73, 26.11, 27.54, 38.76, 39.12, 126.83, 129.77, 168.28$.

4.2.4.5. N-Acryloyl-1,6-diaminohexane hydrochloride[11] (94%, m.p. 164.5–165°C, lit. m.p. [15] ~165°C). Calculated for $C_9H_{19}ON_2Cl$: C, 52.43; H, 9.22; N, 13.57; Cl, 16.99%; found: C, 52.06; H, 9.28; N, 13.33; Cl, 17.93%. IR at λ_{max}: 3305, 2946, 2360, 1652, 1620, 1538, 1464, 1402, 1391, 1244, 1229, 999, 979, 791, 678 cm^{-1}. ^1H NMR (D_2O): $\delta = 1.21$ (m, 4H, CH_2), 1.39 (m, 2H, CH_2), 2.82 (m, 2H, CH_2), 3.10 (m, 2H, CH_2), 5.57 (m, 1H, vinyl proton), 6.05 (m, 2H, vinyl protons). ^{13}C NMR (D_2O); $\delta = 24.95, 25.23, 26.36, 27.76, 38.97, 39.18, 126.76, 129.81, 168.21$.

4.2.4.6. N-Acryloyl-1,7-diaminoheptane hydrochloride (92%). IR at λ_{max}: 3404, 3278, 2936, 1652, 1617, 1547, 1475, 1410, 1358, 1239, 1158, 1067, 977 cm^{-1}. ^1H NMR (D_2O); $\delta = 1.18$ (m, 6H, CH_2); 1.38 (m, 2H, CH_2); 1.48 (m, 2H, CH_2); 2.81 (m, 2H, CH_2); 3.08 (m, 2H, CH_2); 5.57 (m, 1H, vinyl proton); 6.05 (m, 2H, vinyl protons). ^{13}C NMR (D_2O); $\delta = 25.20, 25.51, 26.37, 27.51, 27.86, 39.10, 48.64, 126.72, 129.82, 168.16$.

4.3. Polymer synthesis

Standard AB_2 polymerizations were carried out in the melt at 210°C, unless stated otherwise. The temperature of the reaction was ramped at 10°C min^{-1} to 210°C. The reaction times quoted are measured from the onset of 210°C. All experiments are carried out under at constant nitrogen flow with constant stirring at 125 rpm.

4.3.1. Sample polymer characterization

Poly(amidoamine) hydrochloride, prepared from *N*-acryloyl-1,6-diaminohexane hydrochloride, by reaction at 190°C for 240 min.

Calculated for monomer $C_9H_{18}ON_2$.HCl: C, 52.43; H, 8.74; N, 13.59; Cl, 16.99%; found for polymer: C, 51.86; H, 9.47; N, 13.25; Cl, 16.40%. IR at λ_{max}: 3430, 2931, 1651, 1557, 1455, 1384, 1054 cm^{-1}. ^{13}C NMR (D_2O): $\delta = 25.03$, 25.17, 25.34, 26.42, 27.78, 30.91, 38.97, 39.11, 39.24, 43.24, 47.38, 126.78, 129.87, 171.41. ^1H NMR (D_2O): $\delta = 1.10–1.70$ (m, 8H, CH_2); 2.45–3.40 (m, 4H, CH_2); 5.50–6.25 (m, 3H, vinylic protons). (DP = 9.23; extent of reaction = 89.2%; α-value = 0.446; $M_n = 1900$, all calculated from ^1H NMR data.)

Acknowledgements

This work was funded by a ROPA award from the EPSRC Chemistry Committee and the Special Grant to the IRC from the EPSRC Materials Committee. We thank Drs Richard Peace (RHF123G ab initio MO calculations) and Alan Kenwright (NMR measurements) for their practical help and Professors R.H. Grubbs and R.W. Richards for helpful discussions.

References

[1] Vanhee S, Rulkens R, Lehmann U, Rosenauer C, Schulze M, Køhler W, Wegner G. Macromolecules 1996;29:5136. and references therein.
[2] Schlicke B, Frahn J, Schluter AD. Synthetic Metals 1996;83(3):173.
[3] Gong C, Gibson HW. Current Opin Solid State Mater Chem 1997;2 (6):647.
[4] de Brabander-van den Berg EMM, Meijer EW. Angew Chem Int Ed Engl 1993;32:1308.
[5] Fréchet JMJ, Hawker CJ. In: Agarawal SL, Russo S, editors. Comprehensive polymer science, second supplement. Oxford: Pergamon, 1996:chap. 3.
[6] Dagani R. Chem Eng News 1996;June:30.
[7] Tomalia DA, Esfand R. Chem. Ind 1997:416.
[8] Hobson LJ, Harrison RM. Current Opin Solid State Mater Chem 1997;2(6):683.
[9] Hult A, Malmström E. JMS Rev Macromol Chem Phys C 1997;37:555.
[10] Lovell PA. In: Booth C, Price C, editors. Comprehensive polymer science, vol. 1. Oxford: Pergamon, 1989:chap. 9.
[11] Mourey TH, Turner SR, Rubinstein M, Frechet JMJ, Hawker CJ, Wooley KL. Macromolecules 1992;25:2401.
[12] Meijer EW. View expressed in lectures, e.g. EU SELOA Summer School, Siena, Italy, May 1997 and elsewhere.
[13] Flory PJ. J Am Chem Soc 1952;74:2718.
[14] Hawker CJ, Lee R, Fréchet JMJ. J Am Chem Soc 1991;113:4583.
[15] Holter D, Frey H. Acta Polymerica 1997;48:30.
[16] Frey H, Holter D. Acta Polymerica 1997;48:295.
[17] Hobson LJ, Kenwright AM, Feast WJ. Proc. American Chemical Society, Polymeric Materials Science and Engineering Meeting, Vol. 77, Las Vegas, NV, Sept. 1997:220. (First presented at Recent Advances in Polymer Synthesis Meeting, York University, July 1996).
[18] Hobson LJ, Kenwright AM, Feast WJ. J Chem Soc Chem Commun 1997:1877.
[19] Tomalia DA, Naylor NA, Goddard A. Angew Chem Int Ed Engl 1990:138.
[20] Jacobson AR, Makris AN, Sayre LM. J Org Chem 1987;52:2592.
[21] Krapcho AP, Kuell CS. Synth Commun 1990;20:2559.
[22] Stahl GL, Walter R, Smith CW. J Org Chem 1978;43:2285.
[23] Greene TH, Wutts PGM. Protective groups in organic synthesis, 2nd. edn. New York: Wiley.
[24] Doggrell DM, Pegg DT, Bendall MR. J Magn Reson 1982;48:323.
[25] Percec V, Chu P, Kawasumi M. Macromolecules 1994;27:4441.
[26] Chu F, Hawker CJ, Pomery PJ, Hill DJT. J Polym Sci Part A, Polym Chem 1997;35:1627.
[27] Feast WJ, Keeney AJ, Kenwright AM, Parker D. J Chem Soc Chem Commun 1997:1749.
[28] This concept was first suggested by Professor R.H. Grubbs (California Institute of Technology).
[29] We thank Dr Richard J. Peace (IRC) for these calculations.
[30] Jackson C, Simonsick WJ Jr. Current Opin Solid State Mater Chem 1997;2(6):661.
[31] Dey M, Castoro JA, Wilkins CL. Anal Chem 1995;67:1575.
[32] Feast WJ, Hamilton LM, Hobson LJ, Ranard S. J Mater Chem, submitted.
[33] Feast WJ, Parker D, unpublished results.
[34] Van genderen PHB, Baars MWPL, Elissen-Roman C, de Brabander-van den Berg EMM, Meijer EW. Proc Am Chem Soc Polym Mater Sci Eng 1995;73:336.
[35] Martin K, Spickermann J, Rader HJ, Mullen K. Rapid Commun Mass Spectrom 1996;10:801.
[36] Jackson AT, Yates HT, MacDonald WA, Scrivens JH, Critchley G, Brown J, Deery MJ, Jennings KR, Brookes C. J Am Soc Mass Spectrom 1997;8:132.
[37] Dogruel RW, Nelson RW, Williams P. Rapid Commun Mass Spectrom 1996;10:1471.
[38] Kricheldorf HR, Lohden G, Stober O. Polym Prep 1995;36:749.
[39] Miller TM, Kwock EW, Neenan TX. Macromolecules 1992;25:3143.
[40] Kumar A, Ramakrishnan S. J Polym Sci, Part A: Polym Chem 1996;34:839.
[41] Feast WJ, Keeney AJ, personal communication.
[42] Turner SR, Walter F, Voit BI, Mourey TH. Macromolecules 1994;27:1611.
[43] Fréchet JMJ, Hawker CJ. React Funct Polym 1995;26:127.
[44] Malmström E, Johansson M, Hult A. Macromolecules 1995;28:1698.
[45] Malmström E, Hult A. Macromolecules 1996;29:1222.
[46] Feast WJ, Stainton NM. J Mater Chem 1995;5(3):405.
[47] Tomalia DA, Hedstrand DM, Wilson LR. Encyclopaedia of polymer science and engineering, 2nd edn. New York: Wiley, 1990:46.
[48] Hobson LJ, Feast WJ. J Chem Soc Chem Commun 1997:2067.